NUMERICAL STUDY OF LARGE SCALE STRUCTURE FORMATION OF THE UNIVERSE

A project report submitted to Manipal University for partial fulfillment of the requirement for the award of the degree of

MASTER OF SCIENCE

In

Physics

Submitted by

FIONA SHALOM DMELLO

Reg. No. 153103007

Under the guidance of

Dr. Kazuyuki Furuuchi
Manipal Centre for Natural
Sciences (MCNS)
Manipal University
Manipal

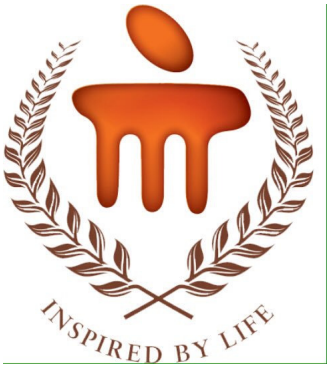

MANIPAL UNIVERSITY

MANIPAL – 576104, KARNATAKA, INDIA

DEPARTMENT OF SCIENCES

MANIPAL UNIVERSITY

MANIPAL – 576 104 (KARNATAKA), INDIA

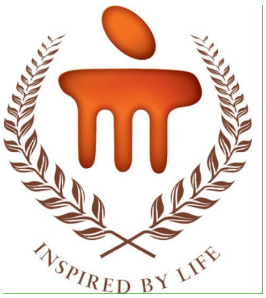

MANIPAL

APRIL 2017

CERTIFICATE

This is to certify that the project titled **Numerical Study of the Large Scale Structure of the Universe** is a record of the bonafide work done by **Fiona Shalom D'Mello** (Reg. No. 153103007) submitted for the partial fulfilment of the requirements for the award of the Degree of Master of Science (MSc) in **Physics** of Manipal University, Manipal, Karnataka, during the academic year 2016 – 17.

Dr. Kazuyuki Furuuchi
Project Guide
Manipal Center for Natural Sciences(MCNS)
Manipal University

Dr. Vyasa Upadhyaya
Head of the Department
Department of Physics
M.I.T. Manipal

Prof. Dr. Padmalatha
Coordinator, Department of Sciences
Manipal University

Acknowledgement

The opportunity to work at MCNS first came as an unexpected blessing to me. Dr. Kazuyuki and Dr. Debbijoy, I shall always be grateful for the (almost) four hours long conversation that we had on the day we first came to MCNS, and for the many more hours that I got to spend learning under your guidance, thereafter. I especially thank Dr. Kazuyuki, for accepting me as your student and letting me learn under your patient and kind guidance. I would not have come so far if it wasn't for your open-mindedness and steady support throughout the year.

Noel Jonathan, thank you for helping me out at all times. From the beginning of the SRI, till the very end. Having you for a collegue made this experience a lot more educational and enjoyable.

Without naming anyone in particular, I thank all the other mentors and scholars at MCNS for your careful and positively constructive criticism at the talks that were arranged for our benefit.

I would like to thank my family. Especially my brother Rolan, for having helped me learn Python. I could keep writing about how wonderfully loving you guys have been. But all those words would just seem superfluous.

I have my classmate to thank for having introduced me to everyone at MCNS. I shall always remember the heat and the jittering nervousness, of that summer morning she dragged me to MCNS as she kept explaining why we should still consider applying for the internship, a week after the last date for the submission had already passed. Thank you Meghashree!

Abstract

With data from galaxy surveys, it is possible to map the three dimensional distribution of galaxies. Galaxy distribution provide information about distribution of mass in the early universe which consequently help us understand the evolution of the universe. On a scale of billion light years, galaxy distribution show what is called the 'Large Scale Structure' (LSS) of the universe. Theoretical models are proposed to explain how LSS was formed. One such conceptual model is the 'Origami model' proposed by Dr. Mark Neyrinck [1]. The objective of this project undertaken is to examine the validity of this model by means of testing an approximation that needs to be satisfied in order to be able to apply this model for cosmological structure formation studies.

List of Figures

Contents

Chapter 1

Introduction

Galaxies are not uniformly distributed all over the Universe. Today, the Sloan Digital Sky Survey (SDSS) is the largest collaborative effort aimed at collecting and studying data concerning an enormous sample of galaxies around us. Such 'Galaxy Surveys' can map the three dimensional distribution of galaxies. Galaxy distributions, contain a lot of information about the history of the Universe. Galaxy distribution also show the existence of what is referred to as the Large Scale Structure of the Universe(LSS) and gravity is what governs the formation of Large Scale Structure of the Universe. More than a 100 billion galaxies are observed in the LSS. The 'Large Scale' at which these structures are observed is in the order of a billion light years.

In order to study and understand the reason for formation of these structures or try to classify the structures formed, one needs to keep a close eye on galaxy distribution and its evolution over large scales of time. What leads to the formation of LSS cannot be satisfactorily studied with just the observational data from Galaxy surveys alone. Theoretical models are proposed to explain how these structures could have come into being. But these models need to be tested to see how well predictions made based on them fit-in with the observational data that has been collected by means of Galaxy Survey. This of course, is not a straight-forward job and requires understanding and clever use of computational power and techniques that we currently have. Thus, computational techniques are used to theoretically understand the LSS formation of the universe.

Chapter 2

Background and Literature Review

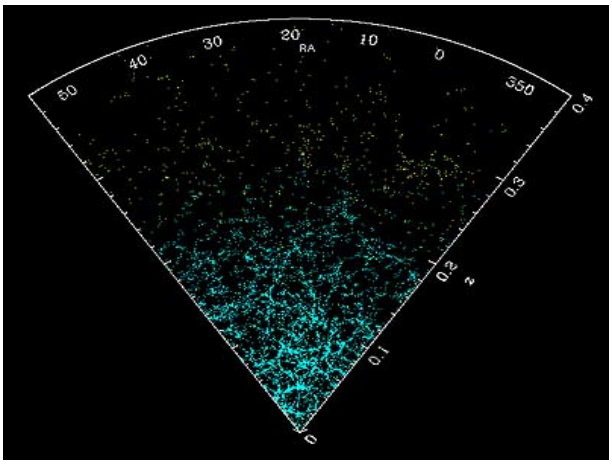

Figure 2.1: The lumpy modern universe revealed by galaxy surveys
A 2D picture of galaxy distribution as obtained from Sloan Digital Sky Survey(SDSS) database. Source:http://skyserver.sdss.org/dr12/en/sdss/discoveries/discoveries.aspx

2.1 The large scale structure of the universe

The Big Bang Model of Cosmology is the leading explaination of how the universe began. According to this model the universe began with a rapid expansion of space. The success of this theory is based on three major observations:

- The Hubble's diagrams that directly indicate the expansion of the universe.

- The abundance of light elements, which is in accord with the predictions of Big Bang Nucleosynthesis (BBN).
- The Cosmic Microwave Background (CMB) radiation with anisotropies in it.

The implications of the results obtained from the Hubble's diagrams when extrapolated backward is that the universe, in its early stage was dense, hot and almost very much the same as everywhere else. That is, matter and radiation in the early universe existed in the form of a hot plasma occupying a small region of space. CMB is radiation that exists everywhere and is left over from when the universe was nearly 300,000 years old. The anisotropies in the CMB tell us that the cosmic plasma had small mass-energy density inhomogeneities/perturbations with a characteristic spectrum , which are widely believed to be the seeds that led to the formation of the Large Scale Structures in the universe. The anisotropies are as small as one part in 10^5 on an average [2]. This means that the early universe consisted of matter and radiation that were distributed in an isotropic and remarkably homogeneous manner. Remarkably homogeneous because, as previously mentioned, the density inhomogenieties in their distribution were very small (For more details, please refer [3], [4], [5]).

The universe today is neither homogeneous nor isotropic. We see galaxies containing hundred billion stars spewed all over. We also see a large number of galaxies themselves clustering to form 'galaxy clusters' in some regions. These galaxies and clusters of galaxies constitute what we call 'Structure'. On scales as large as a billion light years, these 'Structures' themselves create structures of different kinds - walls, voids or filaments, which is aptly named the 'Large Scale Structure (LSS) of the Universe' [4]. A large number of surveys of galaxies were designed since the 1980's in order to be able to observe structures in the universe, culminating in two large surveys - Sloan Digital Sky Survey (SDSS) [6] and the Two Degree Field Galaxy Redshift Survey [7], which compile the redshifts of and hence the distance to, a million galaxies. 2.1 and 2.2, are a two dimensional slice of the three dimensional map of the Large Scale Structure of the Universe, done using observational data from the SDSS. Each dot in these figures represents a galaxy. The Large Scale Structure is sometimes also referred to as the 'Cosmic Web' [8].

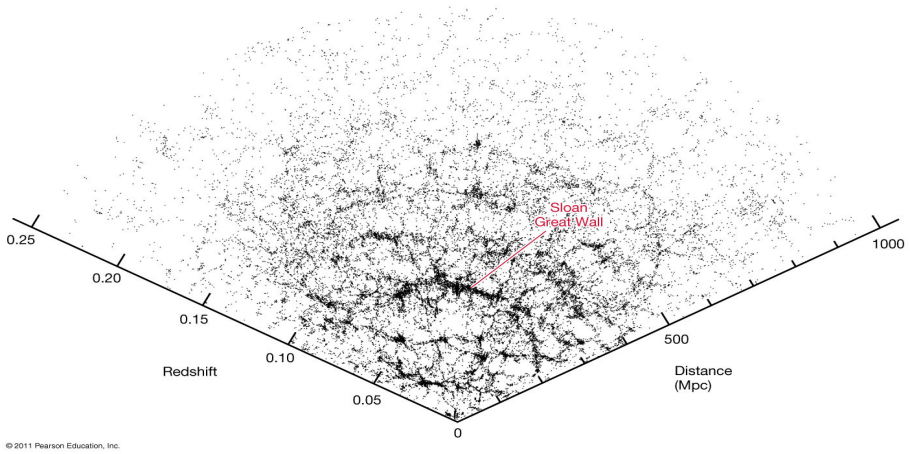

Figure 2.2: Data obtained from SDSS plotted in terms of Redshift and Distance. The Sloan Great Wall is the largest known structure to man, discovered in 2003 through the same data.

Source:http://pages.uoregon.edu/jimbrau/BraulmNew/Chap26/7th/AT-7e-Figure-26-01.jpg

2.2 Dark matter

With the anisotropies in the CMB being very small, the early universe is approximately smooth in terms distribution of mass-energy density. The time evolution of the scale factor a describes the effects of expansion of the universe. The current value of a is set to one. Which means that a was smaller during the early stage of the universe. Thus, scale factor is clearly time dependent and is written as $a(t)$. In addition to this, we also have to consider the geometry of the universe which is both homogeneous and isotropic. Of the three possible geometries (flat, open or closed), a flat universe has energy density equal to a critical value ρ_c. To obtain information about the history of the universe, one must be able to determine the change in scale factor with time. The Hubble rate, described by equation (2.1), is a measure of how quickly the scale factor changes.

$$H(t) = \frac{da/dt}{a}, \tag{2.1}$$

Generally speaking, the Friedmann equation (equation (2.2)) provides a link between the evolution of the scale factor and the energy density of the universe $\rho(t)$.

$$H^2(t) = \frac{8\pi G}{3}[\rho(t) + \frac{\rho_c - \rho_0}{a^2(t)}]. \tag{2.2}$$

where, ρ_0 is the present value of energy density and the critical density ρ_c is given by

$$\rho_c = \frac{3{H_0}^2}{8\pi G} \tag{2.3}$$

where H_0 is the current value of Hubble rate and G is the Newton's gravitation constant. Note that $\rho(t)$ is a sum of several components, each of which vary differently with time. In case of a flat universe, the energy density today would be equal to the critcal density, i.e., $\rho_0 = \rho_c$.

Big Bang Nucleosynthesis (BBN), gives us a measure of baryon density (energy density of ordinary matter), today. It is found that ordinary matter contributes almost 5 percent to the energy density of the universe [9] [10]. But the total mass-energy density comes up to about 30 percent of the critical energy density [9] [10]. This estimate provides compelling evidence for the existence of non-baryonic matter, which is called dark matter. (More details in [3])

Dark matter is a substance that makes up nearly 25 percent of the energy density of our universe [9] [10]. What sets it apart from regular matter (that what we are made of and that with which we interact on a daily basis) is that, dark matter is invisible - Invisible in the sense that it does not undergo electromagnetic interactions, at least at the currently measurable level. As far as we know, interaction of dark matter with itself and with regular matter is only gravitational in nature. Since it is invisible it is very hard to detect and study. However, there are many observational evidences supporting the existence of dark matter and the sheer contribution of dark matter to the mass density of the universe is not ignorable. Why dark matter is of importance to us has to do with the fact that it plays a crucial role in how galaxies form and cluster. This is directly evident from the above mentioned point that dark matter, weighing in at roughly 25 percent of the energy density in the universe, forms a gravitational scaffold that guides the flow of regular matter in forming galaxies and galaxy clusters, which in turn form the basis of the Large Scale Structure of the Universe.

2.3 The origami model

The story of how the universe went from an almost perfectly uniform beginning to its highly structured form today, is a subject of interest and is being carefully studied

and speculated. Such speculations and studies often lead to proposal of models that may explain the LSS formation. Of them, the "Zeldovich Approximation" is a first-order lagrangian perturbation theory [11]. If we imagine matter particles being initial placed on a uniform grid, where they are labelled by Lagrangian coordinates, then based on the Zeldovich approximation the particles will receive a small initial push from the uniform Lagrangian grid and their subsequent motion carries on in the same direction. The approximation predicts the formation of caustics - when particles from two or more different initial locations arrive at the same final location, in the final density field. These caustics are identified with the walls and filaments we find in large-scale structure. This approximation is known to perform well at reproducing the form of the cosmic web, although it breaks down after caustic formation has occurred. In reality, bound structures are formed whereas the Zeldovich approximation simply predicts that particles sail straight through the caustic which consequently evaporates [12]. The Zeldovich approximation thus breaks down after caustic formation, i.e., it fails to provide understanding of structure formation beyond the point where caustics form.

The conceptual 'Origami Model' was proposed by Dr. Mark C Neyrinck [1] in the year 2012. Through this model he proposes that structure formation in the universe proceeds in a manner similar to origami-like folding of paper. Origami, is a Japanese art of folding paper, a 2D material in 3D space, in order to create 3D structures.

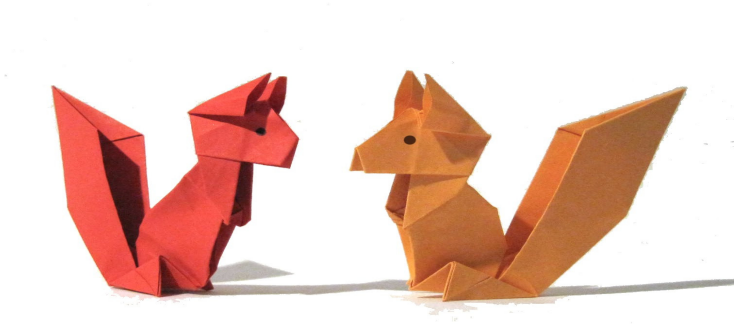

Figure 2.3: Paper Origami

From a flat 2D sheet of paper to a 3D structure.

Source: Origami Time - https://www.youtube.com/watch?v=7DLLpuaS21E

To understand a theory well theorists often consider a simplified model. An extremely

simplified model is called a 'toy model'. As such a toy model, let us consider a universe which only has two spatial coordinates, unlike the real universe which has three spatial coordinates. In a 2D universe, a sheet of paper the size of the universe, pervades all space, i.e., the 'sheet' of paper takes up all the space that exists in such a 2D universe. If this 'sheet' in 2D is folded to form structures in the 2D universe just as the model proposes, then the folding that produce structure would have to be such that the structure does not build up into a third non-existent dimension of the 2D universe. Which is to say, the number of ways in which one is allowed to fold such a 'sheet' in a 2D universe is greatly restricted to certain kinds of folding that allow structure formed to be two dimensional only. This important restriction that appears when we apply the idea proposed in the origami model to a 2D 'sheet' in a 2D universe implies that the type of origami foldings that are of interest to us in scope of applying this model to LSS formation come from a certain subclass of the Japanese art of origami which is referred to as 'flat origami'.

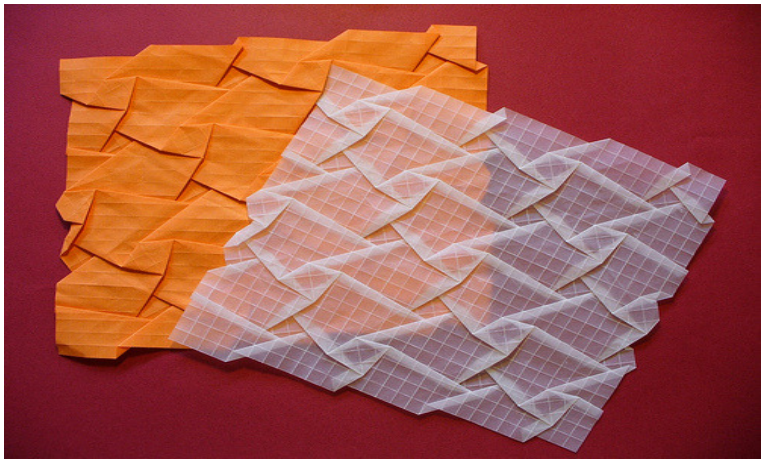

Figure 2.4: Flat Origami

Source: https://www.flickr.com/alebeberorigami/origamitessellations/

When we apply the concepts of this model to our 3D universe, we have to consider a 3D 'sheet' of dark matter (analogous to the 2D sheet of paper in the 2D universe) which pervades all of space. This 3D 'sheet' is initially flat; i.e., made of dark matter that is homogeneously and isotropically distributed. Dr. Neyrinck proposes that gravity folds such a 3D sheet of dark matter, in a manner similar to different kinds of folding made to a paper sheet in flat origami.

In order to be able to apply this analogy of flat origami to cosmological structure for-

mation, there are certain approximations that need to be satisfied. Of these, one approximation is that the sheet of dark matter does not stretch, for a close analogy to paper origami. This approximation means that the sheet of matter, as it folds in space, should not undergo any stretching so as to not cross itself or tear [13]. The objective of this project undertaken is to test the validity of this model through this particular approximation. How we go about doing this will be discussed in the later chapters. The important feature that makes testing the validity of the origami model worth it is that, if the model is found to be valid under certain acceptable conditions, it can give us an idea of how the process of structure formation proceeds after caustic formation has occurred, unlike the Zeldovich approximation. In addition to this, the model can also help classify structures that form (locally), based on the different ways in which the dark matter distribution can fold under the restrictions imposed upon it by the approximations of the model.

Keeping in consideration that dark matter provides greater contribution to total mass-energy density of the universe compared to baryonic matter, we treat galaxies (baryonic matter) and their clusters as tracers of dark matter and assume that dark matter will majorly constitute the 3D sheet of matter that will be folded up according to the approximations of the Origami Model. Our knowledge of dark matter is very limited, yet we have to make use of what we know in order to learn more about how its existence influences structure formation in the universe. Computers allow us to simulate the gravitational dynamics of dark matter in a virtual universe. This is done using an N-particle code wherein the physics of Newtonian gravity will be employed. A detailed discussion on this will be presented in the next section.

This set-up can be crudely used to calculate the trajectories of dark matter particles in our universe. Note that a 'dark matter particle' mentioned here, is not an actual fundamental particle but is a mass element - a pointlike parcel of mass, needed for the simulation. This is how we discretize (represent a continuous system, like dark matter or fluid, using finite amount of data) the dark matter, bringing it from a smooth distribution of mass in our universe to a finite number of mass carrying elements that a computer can manage (refer to section 3.2 for further discussion).

Chapter 3

Methodology

3.1 The N-particle problem

An N-particle problem is defined as a system that contains N number of particles and whose individual positions are to be found (and kept track of) at each instant of time, given a time scale, knowing the initial conditions of all the particles of the system at the first instant of the time scale chosen. By treating matter that causes LSS formation as particles, we can have a N-particle system. And this could help us understand the reason for the formation of LSS.

3.1.1 Gravitational acceleration in a one dimensional universe

In a three dimensional space with a point source, gravitational force is proportional to $\frac{1}{r^2}$. Considering the simplest case of motion possible for particles of the N particle system, we decide to restrict the motion of the particles to only one dimension. This is equivalent to studying the N particle system in a virtual universe made of only one spatial dimension. But the form of the gravitational force in a one dimensional universe is unknown to us. It can however, be found by modeling a situation in three dimension that can be likened to a case of one dimensional gravitational interaction between particles.

For this, let us consider, in a three dimensional space, two sheets of matter with a uniform mass density distribution, i.e, the mass density at each point on a sheet is a constant, which we shall here denote by the symbol μ. These sheets are placed parallel

to each other in the XY plane. In order to understand the situation a little more easily, we say that the matter that makes up a sheet of uniform mass density distribution, can be imagined to be particles of mass M occupying the grids of a mesh. This idea can be applied only if - for μ = constant,

$$\lim_{\Delta x \to 0} and \lim_{\Delta y \to 0}$$

and the mass m scales as a product of Δx and Δy (because $\mu = \frac{m}{\Delta x \Delta y}$).

Assuming this condition to be true for our case of the two sheets in the XY plane with uniform mass density distribution we now consider two meshes instead of two sheets of matter. We name the two meshes A and B as shown in figure 3.1 Let the mass of each particle at each grid point of mesh A be m_a and that on mesh B be m_b. The two meshes are separated from each other by a distance R. Let us now consider a grid point on mesh A, which is to be the origin of this system. The position vector $\vec{R} = R\hat{k}$,where $\hat{k}$ is the unit vector along the positive Z direction, describes the position of particle of mass m_b at a grid point on mesh B.

$$\vec{r'}(x, y) = x\hat{i} + y\hat{j}$$

represents the position vector of any particle of mass m_a at any grid point on mesh A, with magnitude x along the X direction and y along the Y direction. For ease of calculation, we use spherical polar coordinates to describe the position of any particle of mass m_a on mesh A. Then the particle at P on mesh A is described by P$(\vec{r'}, \theta', \phi')$. Note that θ' is ninety degree, for all particles on this mesh as a result of which $d\theta'$ will always be zero. As we speak of sheet like distribution of mass on mesh A and mesh B, the area element of the mesh A will be

$$dw = dr'r'sin\theta' d\phi'$$

which, in our case reduces to

$$dw = r'dr'd\phi'. \tag{3.1}$$

We define the mass distribution of sheet A, μ_A as the mass per unit area of the mesh. That is,

$$\mu_A(r', \theta', \phi') = \frac{m_a}{\int\int r'dr'd\phi'}. \tag{3.2}$$

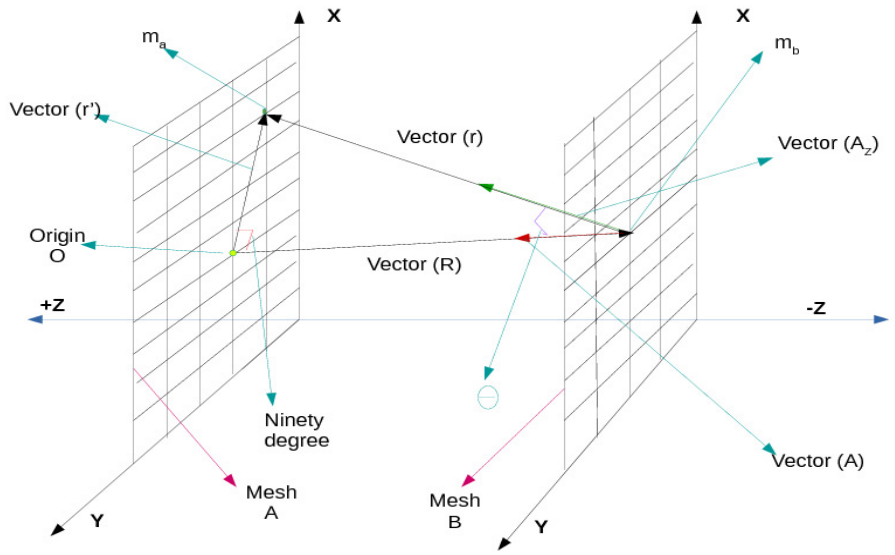

Figure 3.1: Two meshes with particles that interact gravitationally.

As shown in the figure $\vec{r}$ is the vector that goes from particle of mass m_b to mass m_a. See figure 3.1

We also see that,

$$\vec{r} = \vec{r'} - \vec{R} = \vec{x}\hat{i} + \vec{y}\hat{j} - \vec{R}\hat{k}$$

and

$$r = \sqrt{x^2 + y^2 + R^2}.$$

Then the gravitational force acting on any one particle on mesh B, $\vec{F}_B$, due to gravitational interaction with the particle at P on mesh A is given by

$$\vec{F}_B = m_b \vec{A}_B,$$

where $\vec{A}_B$ is the gravitational acceleration experienced by a particle on mesh B due to gravitational interaction with particle P on mesh A, which is given as:

$$\vec{A}_B = G \int_{allspace} \frac{\mu_A r' dr' d\phi'}{r^2} \hat{r} \tag{3.3}$$

where G is the newtonian constant of gravitation of value 6.67408×10^{-11} in $m^3 \cdot kg^{-1} \cdot s^{-2}$ and $\hat{r}$ is the unit vector along $\vec{r}$. When the net effect of the gravitational acceleration of particle on mesh B due to each particle on mesh A is calculated, only the Z-component

of the gravitational acceleration A_{Bz} survives, as all other components get cancelled . This Z-component of gravitational acceleration is

$$A_{Bz} = A_B cos\theta \tag{3.4}$$

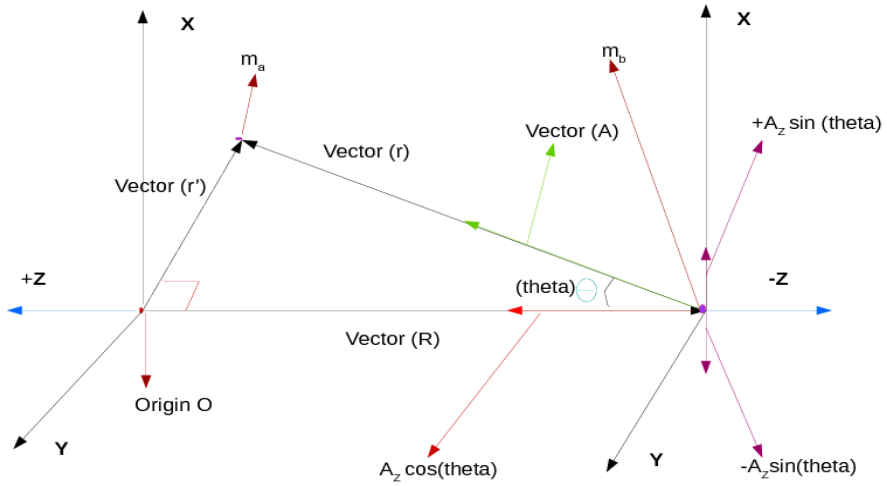

Figure 3.2: Detailed description of two particles on the two meshes interacting gravitationally.

where θ is the angle made by $\vec{R}$ with $\vec{r}$ as shown in 3.1. From 3.2 we obtain

$$cos\theta = \frac{R}{r} = \frac{R}{\sqrt{x^2 + y^2 + R^2}}. \tag{3.5}$$

Thus, we can write,

$$\vec{A}_B = G \int_0^\infty \int_0^{2\pi} \frac{\mu_A cos\theta r' dr' d\phi'}{r^2} \tag{3.6}$$

or,

$$A_B = G\mu_A \int_0^\infty \int_0^{2\pi} \frac{R r' dr' d\phi'}{\sqrt{x^2 + y^2 + R^2}(x^2 + y^2 + R^2)}$$

$$A_B = 2\pi G\mu_A \int_0^\infty \frac{R r' dr'}{(R^2 + r^2)^{\frac{3}{2}}},$$

which can be written as,

$$A_{Bz} = 2\pi G\mu_A \int_0^\infty \frac{r' dr'}{R^2(1 + (\frac{r'}{R})^2)^{\frac{3}{2}}}.$$

On substituting

$$s = \frac{r'}{R}$$

from which we obtain,

$$dr' = Rds,$$

we can write

$$A_B = 2\pi G\mu_A \int_0^\infty \frac{sds}{(1+s^2)^{\frac{3}{2}}}$$

on solving and applying the relevant limits we finally obtain,

$$A_B = 2\pi G\mu_A. \tag{3.7}$$

Equation (3.7) gives us the magnitude of gravitational acceleration experienced by any mass on mesh B due to the collective gravitational action of all particles on mesh A. A_B, as can be clearly seen, is a constant. Thus, the situation wherein two infinitely large sheets, parallel to each other in three dimensional space interact gravitationally, behave in a manner that can be likened to gravitational interaction between two particles along one dimension. The overall effect of this interaction is that the two sheets in three dimensional space move toward each other along the Z axis. An N particle system in a one dimensional universe interacting gravitationally will then be the same as N inifinitely large sheets arranged parallel to each other in three dimensional space, interacting gravitationally. If the sheets are arranged parallel to each other along the YZ plane, then the motion of the sheets is along the X axis of the coordinate system. Here, each sheet corresponds to one particle in one dimensional universe. Thus a system in three dimensions, consisting of N sheets of uniform mass density arranged parallel to each other and interacting gravitationally is equivalent to a system of N particles interacting gravitationally in a one dimensional universe.

With information about the form of gravitational acceleration in a one dimensional universe in hand, our discussions from this point onwards will be along that of a one dimensional gravitational N-particle system.

3.1.2 Gravitational N-particle system

The underlying dynamics relevant for a system of N particles interacting gravitationally is typically the Newton's law of motion. We are now dealing with a N particle system

in a virtual universe one spatial dimension - positions along which are represented by the coordinate x. If i is the index representing a particle being acted upon by the gravitational force from another particle of index j, then the gravitational interaction of any one i^{th} particle of the system with the other particles of the system can be described as,

$$m_i \frac{d\vec{v}_{ij}}{dt} = \sum_{i \neq j, j=1}^{N} \vec{F}_{ij} \tag{3.8}$$

where $\vec{F}_{ij}$ is the vector representing the force acting on the i^{th} particle due to its gravitational interaction with the j^{th} particle. Both the indices, i and j can take values 1,2,3...,N. Here,

$$\vec{v}_{ij} = \frac{d\vec{x}_i}{dt}. \tag{3.9}$$

Here, $\vec{x}_i$ is the position vector of the i^{th} particle. On substituting equation (3.9) in (3.8), we obtain,

$$m_i \frac{d^2\vec{x}_i}{dt^2} = \sum_{i \neq j, j=1}^{N} \vec{F}_{ij}$$

$$m_i \frac{d^2\vec{x}_i}{dt^2} = \sum_{i \neq j, j=1}^{N} m_i \vec{a}_{ij}$$

which gives us,

$$\frac{d^2\vec{x}_i}{dt^2} = \sum_{i \neq j, j=1}^{N} \vec{a}_{ij}. \tag{3.10}$$

Consider $\vec{a}_{ij}$ - the gravitational acceleration produced in particle i due to its interaction with particle j. Equation (3.7) gave us the form of the magnitude of gravitational acceleration, based on which we can write

$$a_{ij} = 2\pi G \mu_j \tag{3.11}$$

where, based on the derivation in section 3.1.1, μ_j is the mass density distribution of the j^{th} sheet in the three dimensional equivalent picture of our one dimensional system. We can simplify equation (3.11) by substituting for μ_j from (3.2), to get

$$a_{ij} = 2\pi \tilde{G} m_j \tag{3.12}$$

where,

$$\tilde{G} = \frac{G}{\pi \bar{r}^2}$$

since, from (3.2)

$$\int_0^{\bar{r}} \int_0^{2\pi} r' dr' d\phi' = \pi \bar{r}^2$$

where, $\bar{r}$ is the magnitude of the position vector of a particle on mesh j which is in the neighborhood of the particle at the origin.

To obtain information about direction of the gravitational acceleration produced, we consider

$$\frac{(x_j - x_i)}{((x_j - x_i)^2)^{\frac{1}{2}}} \tag{3.13}$$

Thus,

$$\vec{a}_{ij} = 2\pi \tilde{G} m_j \frac{(x_j - x_i)}{((x_j - x_i)^2)^{\frac{1}{2}}} \tag{3.14}$$

Substituting equation (3.14) in (3.10) we get,

$$\frac{d^2 \vec{x}_i}{dt^2} = \sum_{i \neq j, j=1}^{N} 2\pi \tilde{G} m_j \frac{(x_j - x_i)}{((x_j - x_i)^2)^{\frac{1}{2}}} \tag{3.15}$$

A second order differential equation can be written as a set of two first order equations. For sake of simplicity and ease, we rewrite the second order differential equation (provide number)of the i^{th} particle as

$$\frac{d\vec{x}_i}{dt} = \vec{v}_{ij}, \tag{3.16}$$

$$\frac{d^2 \vec{x}_i}{dt^2} = \frac{d\vec{v}_{ij}}{dt} = \sum_{i \neq j, j=1}^{N} 2\pi \tilde{G} m_j \frac{(x_j - x_i)}{((x_j - x_i)^2)^{\frac{1}{2}}}. \tag{3.17}$$

Thus for a system containing N particles, there would be a total of N second order differential equations with $2N$ initial conditions (N-initial position and N-initial velocity), that can be transformed and written as a set of $2N$ first order differential equation, which can be solved with the same initial conditions. This transformation corresponds, in theoretical mechanics, to the Hamiltonian mechanics of the equation of motion.

At this point, it is important to note that the equation describing the acceleration of the particle shows us that it depends on the position vectors and masses of all particles of the system, other than itself, at any instant of time. Analytically solving such coupled equations, for a system of particles with N greater than two in general, is proven to be impossible. Not to mention the fact that for a system with N particles, there will be N number of second order differential equations of a similar form that needs to be solved.

For this reason, we rely on computers to help us solve the differential equations of the N-particle system (further discussion in section 3.2).

Now, it is clearly evident from (3.17) that there is a posibility of occurence, at some point of time, of $x_i = x_j$ when the equation of motion of the i^{th} particle of the system is solved. If and when this happens the denominator in equation (3.17) will become zero. This means that, as the distance of separation between two gravitationally interacting particles approaches zero, the gravtational acceleration experienced by one particle due to the other will grow infinitely larger. This will make further computational calculations very difficult as computers cannot handle the concept of infinity. In order to avoid this singularity that may arise during calculations, a small approximation is made to the gravitational acceleration, by adding a very small non-zero force softening factor α^2 to the denominator and leading us to change the equation of motion as shown below

$$\frac{d\vec{x}_i}{dt} = \vec{v}_{ij}, \tag{3.18}$$

$$\frac{d^2\vec{x}_i}{dt^2} = \frac{d\vec{v}_{ij}}{dt} = \sum_{i\neq j,j=1}^{N} 2\pi\tilde{G}m_j \frac{(x_j - x_i)}{(((x_j - x_i)^2) + \alpha^2)^{\frac{1}{2}}}. \tag{3.19}$$

It is to be noted that this approximation made in order to make the task of computation easier, serves as a source of error, each time a calculation is made using the above equation. The set of equations (3.18) and (3.19) will be solved using numerical approximation methods with appropriate initial conditions to see how the line (dark matter particles form a 'sheet' when they are restricted to move along 2D and form a 'line' when they are restricted to move along 1D) made of dark matter particles behaves when the particles interact gravitationally.

3.2 Numerical approximation methods

In physics, we usually describe physical laws in terms of continuous variables and differential equations. As mentioned at the end of chapter two (section 3.1.2), it is impossible to solve the equations of motion (which contain second order differentials) for a system with N greater than two, analytically. For this reason we choose to rely on computers to help us solve the system of equations. But computers can only deal with discretized

form of variables, and not continuous. Because of this computational limitation, we can only obtain solutions to the differential equations in numerical/discrete forms. The techniques involved in solving differential equations this way are generally called "Numerical Approximation Methods". There are a large variety of Numerical Approximation Methods and as the name suggests, these methods of solving differential equations always provide an approximated solution and not the exact solution. The different methods for numerical approximations usually differ in terms of the order of truncation error that creeps in as a result of approximating the solution to a differential equation and the ease with which one can solve differential equations using a particular method. For the purpose of solving the gravitational N-particle problem, we have chosen to start with the simplest of numerical approximation methods - The Euler's Method.

3.2.1 The Euler's method

Euler's Method is used to approximate solutions to first order differential equations for a set of given initial conditions. In the case of gravitational N-particle problem, we have $2N$ first order differential equations that need to be solved with the help of $2N$ initial conditions that are given to us. We know that for each particles equation of motion we need to solve for the time differential of velocity and time differential of position of that particle. The simplest way to advance the time from t to $t + \Delta t$ is to use the first order approximation:

$$\vec{r}(t + \Delta t) = \vec{r}(t) + \Delta t \vec{v}(t),$$

$$\vec{v}(t + \Delta t) = \vec{v}(t) + \Delta t \vec{a}(t).$$

Where $\vec{a}(t)$, is the the gravitational acceleration produced in the particle when it is acted upon by other particles of the system. Clearly, the error made in each step of this approximation algorithm is $O[(\Delta t)^2]$. There are several ways to proceed to derive more accurate, higher-order integration schemes. But because of the ease with which we can apply the Eulers scheme to the N-particle system, we shall make use of this method.

3.2.2 Euler's method applied to a gravitational N-particle system

At the end of the section 3.1.2, we obtained the equation of motion of a particle when it interacts gravitationally with the other particles of the N particle system in a one dimensional virtual universe, at some instant of time. This system of equations can now be solved by applying the Euler's approximation method mentioned above. The equation of motion of the i^{th} particle of the system interacting with the $N-1$ number of j^{th} particles of the system given below, explicitly shows how the position vector and velocity of the i^th particle are both functions of time.

$$\frac{d\vec{x}_i(t)}{dt} = \vec{v}_{ij}(t),$$

$$\frac{d^2\vec{x}_i}{dt^2} = \frac{d\vec{v}_{ij}}{dt} = \vec{a}_{ij}(t) = \sum_{i\neq j, j=1}^{N} 2\pi\tilde{G}m_j \frac{(x_j - x_i)}{(((x_j - x_i)^2) + \alpha^2)^{\frac{1}{2}}}$$

The position and velocity of the i^{th} particle of the system (on interacting with the $N-1$ number of j^{th} particles) at an instant $t + \Delta t$ of time while its position and velocity at the t^{th} instant of time is known, is obtained by applying the Euler's approximation as shown below

$$\vec{x}_i(t + \Delta t) = \vec{x}_i(t) + \Delta t\vec{v}_{ij}(t),$$

$$\vec{v}_{ij}(t + \Delta t) = \vec{v}_{ij}(t) + \Delta t\vec{a}_{ij}(t).$$

That is,

$$\vec{x}_{ij}(t + \Delta t) = \vec{x}_{ij}(t) + \Delta t\vec{v}_{ij}(t) \tag{3.20}$$

$$\vec{v}_{ij}(t + \Delta t) = \vec{v}_{ij}(t) + \Delta t \sum_{i\neq j, j=1}^{N} 2\pi\tilde{G}m_j \frac{(x_j - x_i)}{(((x_j - x_i)^2) + \alpha^2)^{\frac{1}{2}}} \tag{3.21}$$

Thus knowing the intial conditions, i.e., the values of position and velocity of the particles of the system at an instant t of time and a fixed value of Δt the positions and velocities of the particles of the system can be approximately estimated through the final set of equations (3.20) and (3.21), mentioned above.

Chapter 4

Behavior of Dark Matter Particles

As mentioned in the chapter 2 (section 2.3), the aim of the project is to test an approximation made in the Origami Model, which states that the sheet of dark matter does not undergo strecthing. In order to achieve this aim, we first have to look at how a system of dark matter mass elements (discretization of dark matter distribution because of computational limitations) that interact gravitationally, will behave. To keep our model simple, we shall begin by dealing with systems in a virtual universe of one spatial dimension. This causes our system to be a line-like distribution of dark matter. The behavior of the system will be studied through the phase space plots. Phase space of a system is a plot of the momentum versus position of the particles of the system. Since change in momentum of a particle in our case is directly proportional to the change in velocity of the particle (as the mass does not vary) we will be looking at plots of velocity versus position of the particles of the system.

We have already seen at the end of section 3.1.1 that, a system in a three dimensional universe consisting of N sheets of uniform mass density arranged parallel to each other and interacting gravitationally is equivalent to a system of N particles interacting gravitationally in a one dimensional universe. This means that, each sheet of uniform mass density corresponds to a particle in its corresponding one dimensional picture. Then, to set up a N particle system with a homogeneous mass-energy density distribution we have to see to it that the mass density distribution of not just each sheet but that of the system of sheets in its corresponding three dimensional picture is a constant. Now, from our discussion in section 2.2 , we came across the expression for critcal energy density

ρ_c. This means that the energy density of the currently flat universe ρ_0, is the same as its critical density, i.e.,

$$\rho_c = \rho_0 = \frac{3{H_0}^2}{8\pi G}$$

The current value of $H_0 = 67.3\ km \cdot s^{-1} \cdot Mpc^{-1}$ [9]. Substituting this in the above equation along with $G = 6.673 \times 10^{-11}\ N \cdot m^2 \cdot kg^{-2}$ we obtain the value for energy density for a currently flat universe to be $\rho_0 = 8.67 \times 10^{-27}\ kg \cdot m^{-3}$.

In section 2.2 we also came across the fact that matter, both baryonic (5 percent) and non-baryonic (25 percent), make a total contribution of nearly 30 percent to the total energy density of the universe. Since in the system that we set up it is only mass that contributes to the the total energy density of the system, the total mass-energy density of the system has to be equal to $0.3\rho_0$. Thus for any N particle system that we set up, its mass-energy density has to be equal to $0.3\rho_0 = 2.601 \times 10^{-27}\ kg \cdot m^{-3}$.

Next we decide on number of particles in a box of a fixed length, in order to find what the mass of each particle (mass carried by each sheet of uniform mass density) in the box should be, such that the total mass-energy density of the system is equal to 2.601×10^{-27} $kg \cdot m^{-3}$. For a system containing 101 particles ($N = 101$), if the size of the box is $L = 101$ Mpc (1 Mpc $= 30.6695 \times 10^{21} m$), then using the expression given below

$$0.3\rho_0 = \frac{NM}{L^3} \tag{4.1}$$

the mass of each particle in the system M, can be found. For the system described, M was found to be equal to $0.227 \times 10^{45} kg$.

4.1 Homogenous system of particles

Now to set up a system of particles $N = 101$ particles, each of mass $0.227 \times 10^{45}\ kg$ such that, the mass-energy density of the system is a constant equal to $0.3\rho_0$. The distance between each pair of particles is set to 1 Mpc (as, $\frac{L}{N} = 1$). All this information was encoded into a program written in Python, a scripting computer language. The distance scale was set to be in terms of mega parsec (1 Mpc = 3.26 million light years). The time scale used for the systems time evolution was in the order of 10^6 years (million years (MY)). The Euler's Method was applied to a N-particle system, to solve the set of

equations of motion for each particle of the system, as mentioned in section 3.2.2. The initial velocity of all particles was set to zero and the value of Δt was set to 0.01, which means that each time step corresponds to ten thousand years. Figure 4.1 is a phase space plot for this system in its initial state and figure 4.2 is a phase space plot for the same system at the end of ten million years.

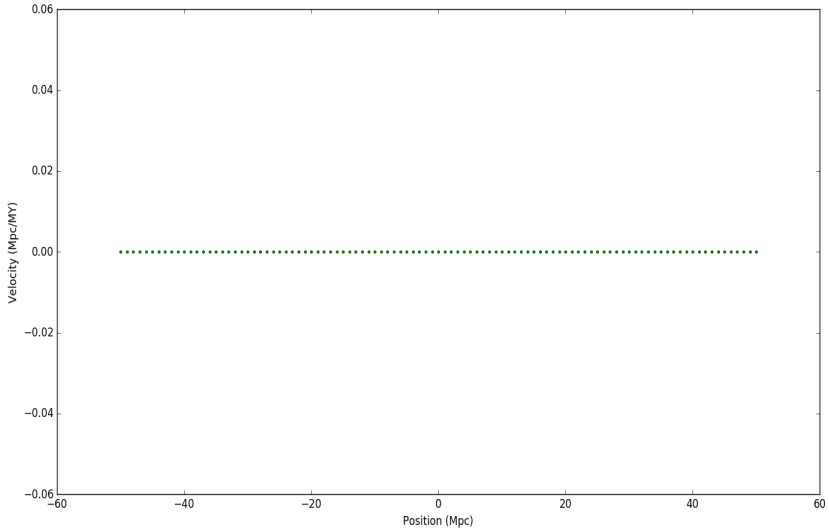

Figure 4.1: Phase space plot of 101 particles system in its initial state.

In figure 4.2, we can see how the system of particles is symmetric in terms of changes in magnitude of both positions and velocities with respect to their initial positions and velocities, but asymmetric in terms of direction of their speeds. We observe that the particles are moving about the centre of mass of the system. The particles at the edge of the system are observed to move much faster than the particles on the inside as there is gravitational force acting on them only from one side. That is, there is no force acting on the particles on the edge from outside the box containing particles and hence there is nothing to hold them back which allows their velocities to change the way we observe it in the plot. Dark matter is a continuous entity that stretchs out infinitely. What we observe in the plot is a result of considering only a finite region of a distribution of dark matter which actually exists beyond the edges of a small region that forms our system and neglecting the effect of the presence of dark matter that exists outside the edges of our system. This point will be taken into consideration and appropriate conditions will be implemented on the system in order to imitate the effect of the presence of dark

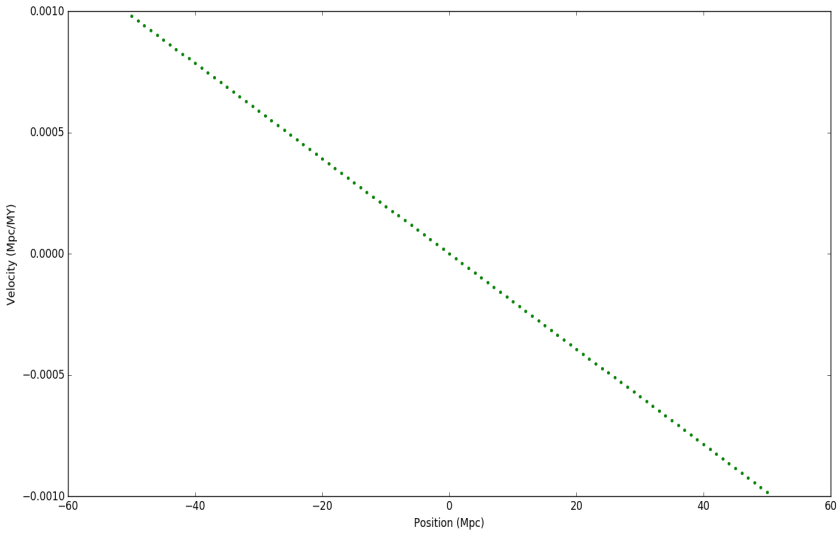

Figure 4.2: Phase space plot of 101 particles system after 10 million years.

matter beyond the edges of the finite region that we will be studying. What conditions and how they are implemented will be discussed in detail in section 4.3.

4.2 System of particles with an inhomogeneity

As mentioned in section 2.1 of chapter 2, the anisotropies in the Cosmic Microwave Background (CMB) indicate that the early universe was not completely smooth [14]. With this information in hand we now will go one step ahead and include a form a inhomogeneity in our test model from the previous section. The inhomogeneity is introduced in the form increased mass density at the centre of our system. This means that the mass-energy density at the centre of the system deviates from the average mass-energy density of the system, which here is equal to $0.3\rho_0 = 2.601 \times 10^{-27}\ kg \cdot m^{-3}$.

This was acheived through the following method: The initial position of the central particle in the system is set to zero. A distance d is then defined as the distance of separation between the central particle and its nearest neighbors on either side. The position of the neighbors of these newly defined particles is then defined by increasing the distance of separation between them from d to

$$d + [l \times d], \tag{4.2}$$

where l is a parameter with which we can vary the mass-energy density distribution in the system. For the described system of particles, l is set to 0.12 or 12 percent. With $N = 101$ particles, since there are 50 particles on either side of the central particle, there will be 49 distances of separation between the 50 particles. If the distance of separation between the last set of particles one edge of the box is set to $\frac{L'=50}{N'=50}\ Mpc$ i.e., $1Mpc$, then the distance separating the central particle from its nearest neighbor is $d = \frac{1}{(1.12)^{49}} = 3.875 \times 10^{-3}\ Mpc$. This procedure is repeated until the position of all the particles in the system is defined. The phase space plot of the initial set up of the system with an inhomogeniety at its centre is as shown in the figure below:

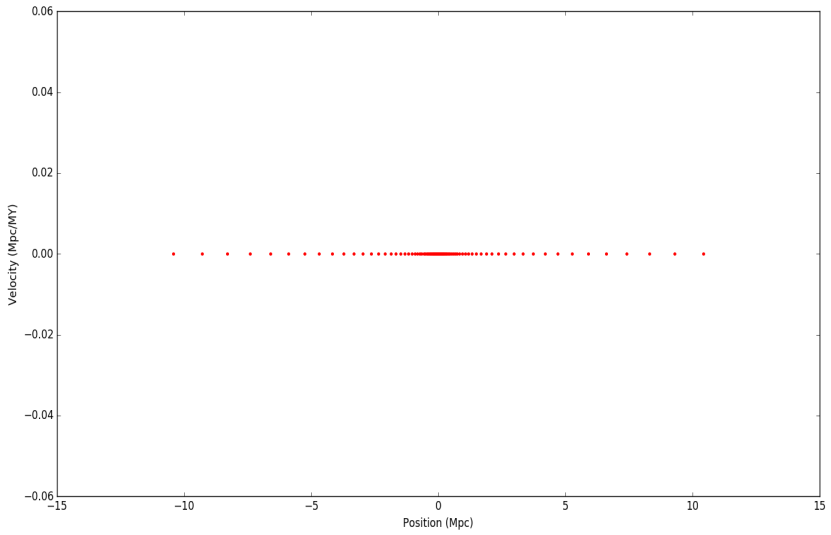

Figure 4.3: Initial set up of the dark matter distribution with an inhomogeneity.

Dark matter distribution, as has been mentioned in section 4.1, is continuous. In order to imitate this continuity we need to reduce the effects of discretization which will be achieved by increasing the number of particles in the toy model at a later stage.

4.3 Conditions at the boundary and implementation of no-stretch approximation

Even though dark matter pervades all space we cannot consider working with infinite number of dark matter mass elements in our computer. Which means that, we have to

implement some conditions in our system, strongly affecting the particles on the edges or boundary of our system, so as to imitate the effect of the dark matter mass elements that we know to exist outside the boundary of our study system.

The condition employed at the boundary for our system consists of a set of dark matter mass elements which will be referred to as "dummy particles". We shall refer to the particles in our study system as "real particles". Each one of the dummy particle carries the same mass as the other particles of the toy model. Dummy particles exist on the outer edge of our study system beyond the last real particle on either side of the study system. Their purpose is to imitate the existence of the continuous dark matter distribution that we know to exist outside the finite system which we have chosen to study, by creating the best possible effects of their existence on our study system (which is but a small part of the dark matter continuum). The number of dummy particles to be included for our study is arbitrarily chosen. The position of each dummy particle is always defined with respect to their nearest real particle. Each dummy particle will at all times maintain a fixed distance separating it from the nearest real particle. As of consequence, the velocities of all the dummy particles will take the same value as that of their nearest real particle at each time step. To put it simply, dummy particles of the system do not obey Newton's law of motion, unlike the real particles of the system. The motion of dummy particles is determined by the conditions that we have imposed on them, as mentioned above. The reason for defining the position of the dummy particles with respect to their nearest real particle is two-fold. First, they will serve to provide the gravtational force that is used to imitate the existence of dark matter outside the system. Secondly, by defining their position at each time step of the computers calculation, with respect to their nearest real particle in a manner as mentioned above, they are made to follow their nearest real particle in terms of position while always maintaining a fixed distance of separation among themselves. This means that the distance between neighboring dummy particles does not ever change which implies that the dark matter sheet in the region occupied by the dummy particles is non strechtable.

The system shown below consists of real and dummy particles in its initial state. The system that was studied consists of a total of 101 particles and the last real particle on either sides in the system is accompanied by 55 dummy particles each.

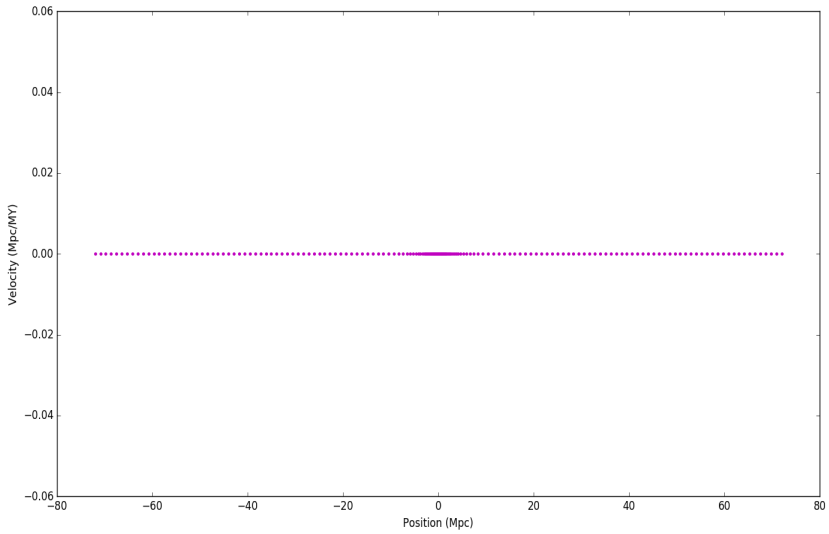

Figure 4.4: Initial set-up of the dark matter distribution with an inhomogeneity along with dummy particles at the boundary of the study system.

By choosing to use conditions mentioned above at the boundary of our study system (system containing only the real particles), we impose the approximation " Dark matter sheet does not stretch for close analogy to paper origami" through our conditions on the dummy particles. We choose to see how exactly, on imposing this approximation on the dummy particles, it effects the behavior of the real particles of the study system.

- Will the line of dark matter distribution in the study system undergo tesselations or foldings clearly visible in its phase space plot?
- Will the distance of separation increase or decrease i.e, will the line of dark matter stretch or compress anytime during the systems evolution with time?
- If yes, by what amount does the line of dark matter stretch or compress?
- Can this amount of strecthing or compression of the dark matter line in the study system be acceptable under the imposition of the no-stretch approximation at the boundaries?

These are some of the questions we shall try to answer through this project.

Chapter 5

Behavior of the System Studied

To summarize the setting up of our toy model, a detailed description of which was given in sections 4.2 and 4.3 of chapter 4, we consider a system to be studied - the study system (contains only real particles), of particles with $N = 101$. The mass of each particle in the system is $M = 0.227 \times 10^{45}\ kg$. For the conditions at the boundary to be applied, we have 55 dummy particles on each edge of our study system. The system contains one inhomogeneity at the centre in the form of an increased mass-energy density distribution in that region created by means of the method mentioned in the previous chapter (section4.2). The position scale for the system is in mega parsec (Mpc) and the time scale is in million years (MY). The value of the speed of light in this system of units is $c = 0.3086\ Mpc \cdot (MY)^{-1}$. The program, written in Python has a total of 1000 time steps. At each time step the system moves ahead by dt = 0.01 million years. So during one run of this program we obtain results on the behavior of the system upto 10 million years. The spacing parameter $l = 0.12$ (equation 4.2) decides the deviation of mass-energy density of the system with respect to the average value of 2.601×10^{27} $kg \cdot m^{-3}$. The initial velocity of all the particles is set to zero. The phase space plots of the system of particles with (first) and without (second) the dummy particles are shown below.

The figure 5.1 is a plot that shows the initial set-up of system of real particles ($N = 101$) and dummy particles (55 on each side) in phase space.

Figure 5.2 is a plot of the initial state of the study system without dummy particles.

While figure 5.3 is a plot that shows the study system with dummy particles at time

slice at the end of one million years.

From figures 5.2 and 5.3, clearly we can see that the particles are moving about the centre of mass of the entire system (comprises of the dummy particles as well). The positions of all particles have not undergone much change but the particles have gained velocities. Figure 5.4 is a time slice of the system (no dummy particles), at the end of one million years.

From figure 5.5, which is the phase space plot of the same study system that has been allowed to evolve for twenty million years, it is evident that the particles with initial negative positions have not had their positions changed by an amount as to make their positions positive in this time slice. Which means that no folding has occurred yet.

Figure 5.6 shows the state of the study system through its phase space plot at the end of eighty million years. Clearly, there has not been any noteworthy change in positions of the particles of the system. But its worth noting that velocity of the particles has been steadily increasing in magnitude over the years.

Figure 5.7 to figure 5.14 are the phase space plots of the study system from 100 to 140 million years. From figures 5.7 to 5.14, as the system evolves in time from a hundred million years to one forty million years, we see that the line-like distribution of dark matter is undergoing folding. Since the particles of the system interact gravitationally only, we can say the gravity folds this line-like distribution of dark matter in a one dimensional universe. It is worth noting that the study system undergoes folding even under the influence of the dummy particles on which the no-stretch approximation of the Origami model has been applied and that the region that at the centre that initially looked densely packed does not look the same as the line-like distribution in the study system folds.

The various phase space plots at different time slices as the system evolved further in time can be see from figure 5.15 to 5.24. In figure 5.19 we see that the line-like distribution of dark matter that started folding at 100 million years is flipping over again at 240 million years. This second continues and becomes more and more apparent as the system evolves in time. This can be clearly seen in figure 5.24, which is the zoomed in image of the phase space plot of the study system at 300 million years.

As the study system undergoes foldings, the spacing between particles at the centre seems

to be visually varying, depending upon the amount by which the line-like distribution has folded. This variation and its implication will be made clear in the next chapter.

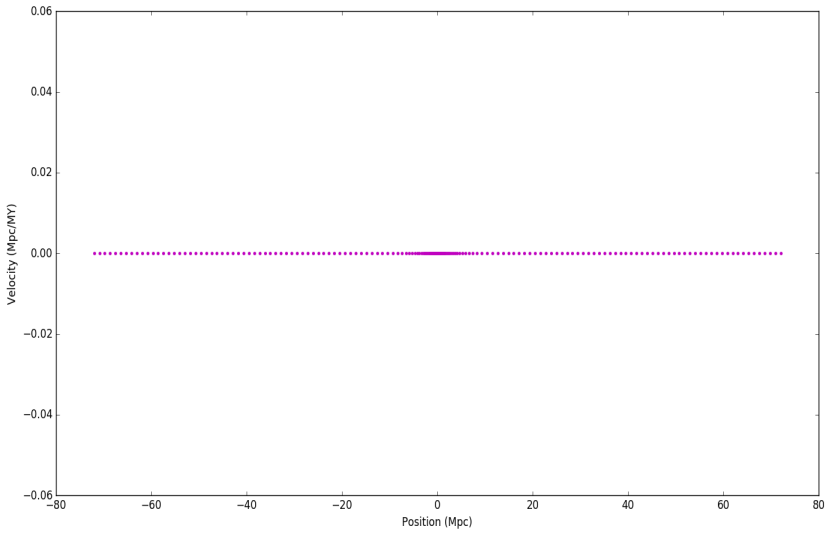

Figure 5.1: Initial set up of the dark matter distribution with dummy particles.

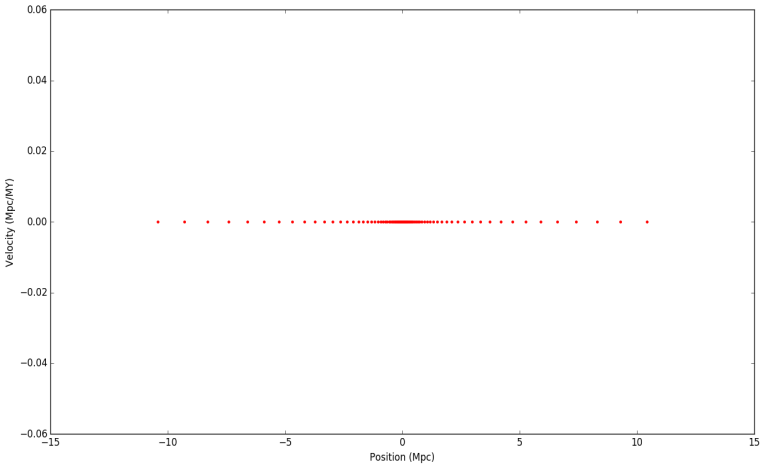

Figure 5.2: Initial set up of dark matter distribution without dummy particles.

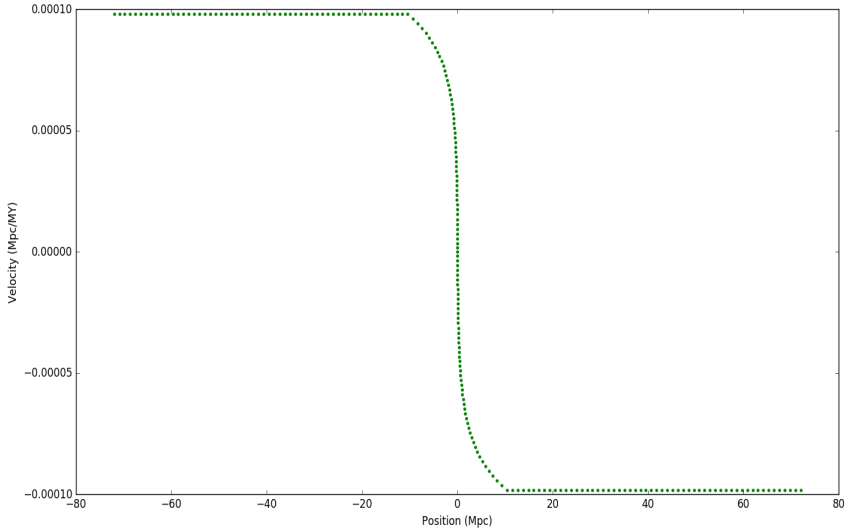

Figure 5.3: Dark matter distribution with dummy particles at 1 million years.

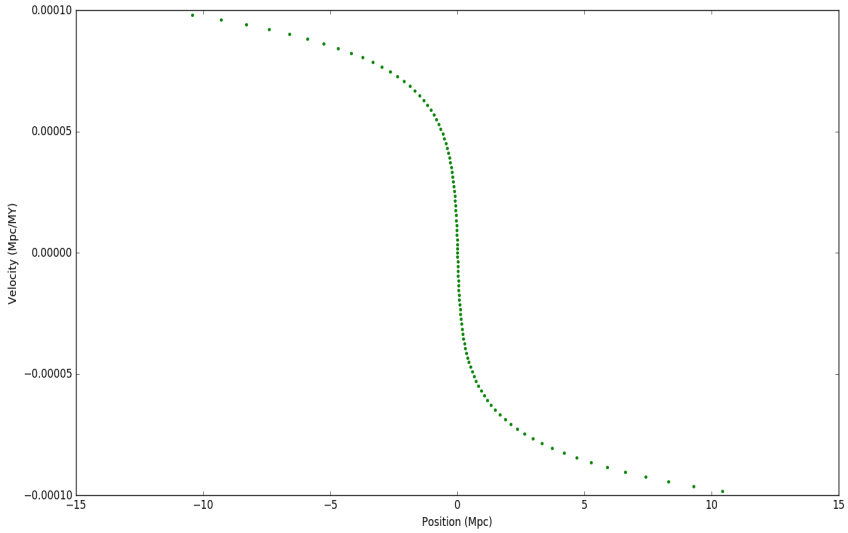

Figure 5.4: Dark matter distribution without dummy particles at 1 million year.

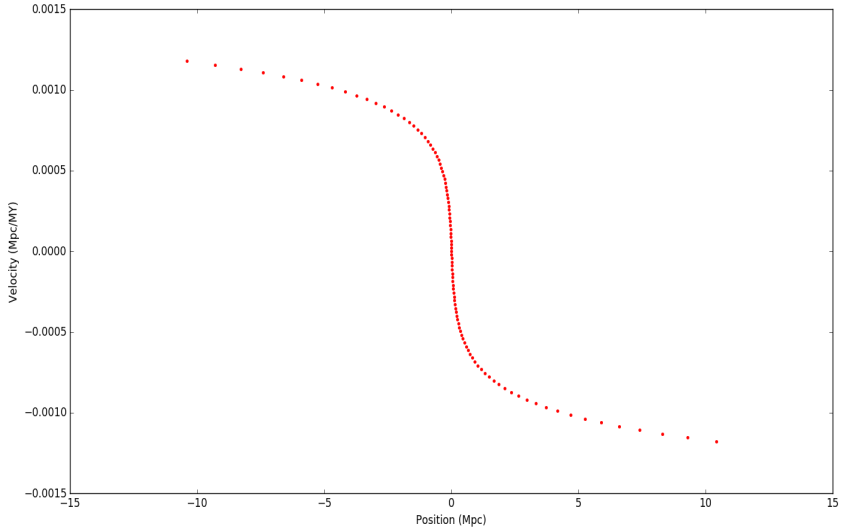

Figure 5.5: Dark matter distribution without dummy particles at 20 million years.

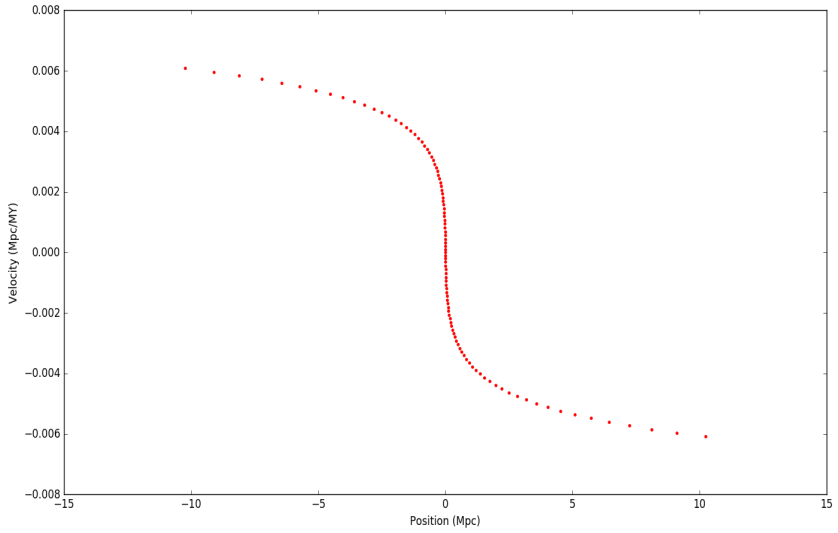

Figure 5.6: Phase space plot of dark matter distribution without dummy particles after 80 million years.

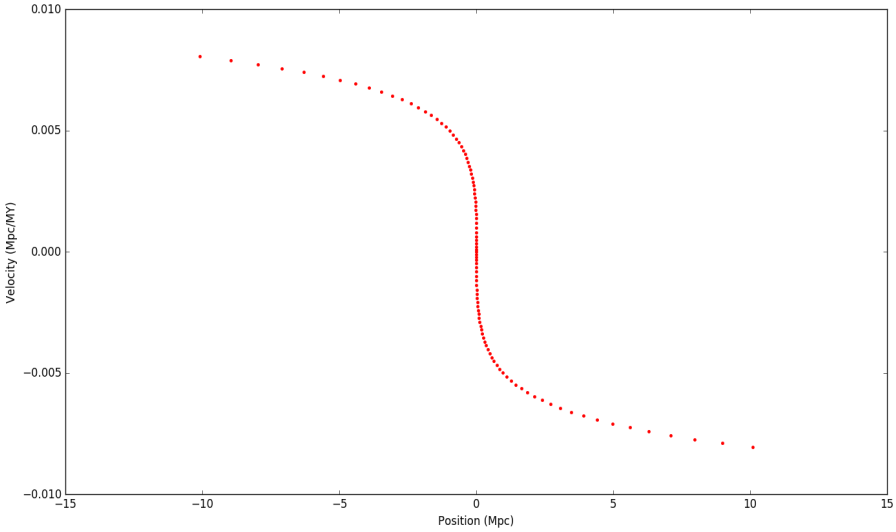

Figure 5.7: The phase space plot of the study system after 100 million years

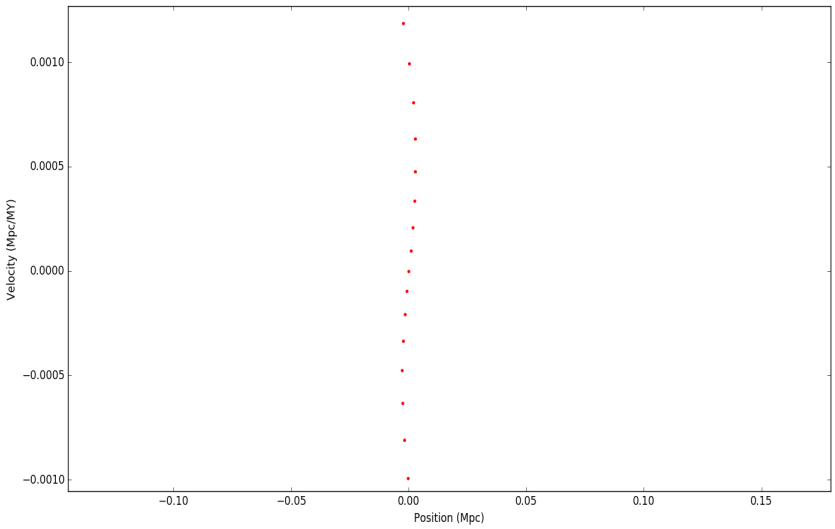

Figure 5.8: Zoomed in image of the study system after 100 million years.

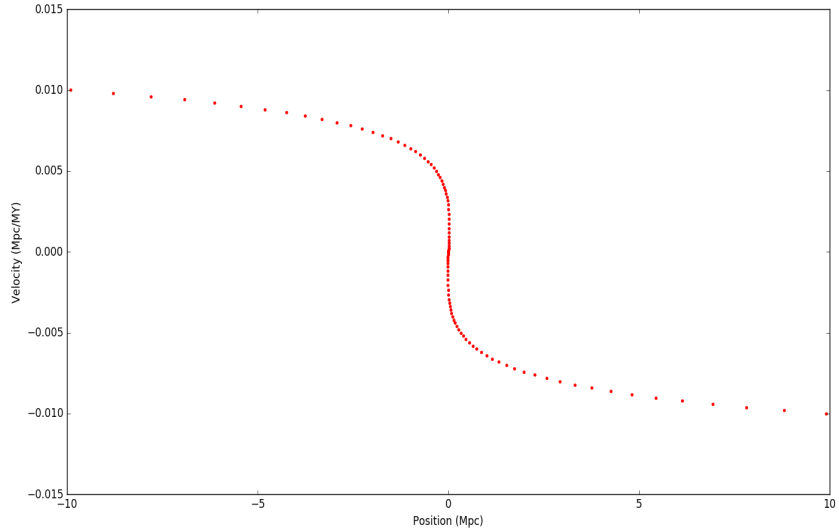

Figure 5.9: Phase space plot of study system after 120 million years.

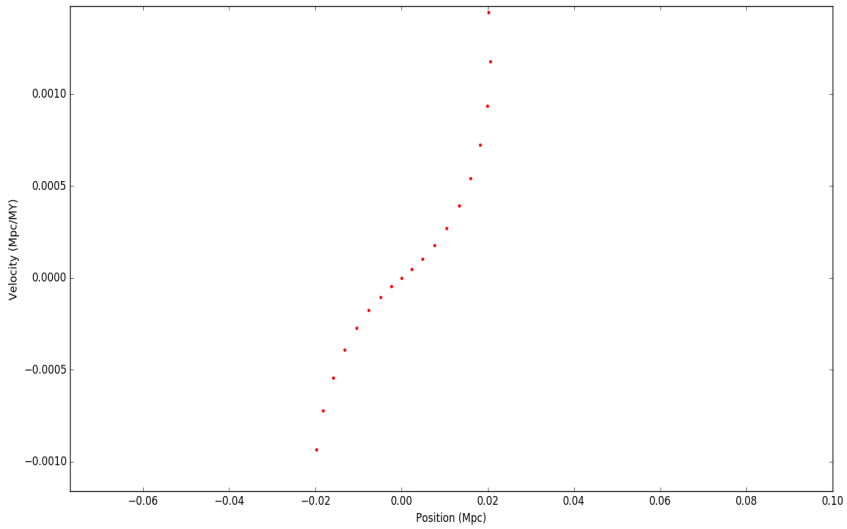

Figure 5.10: Zoomed in image of the study system after 120 million years.

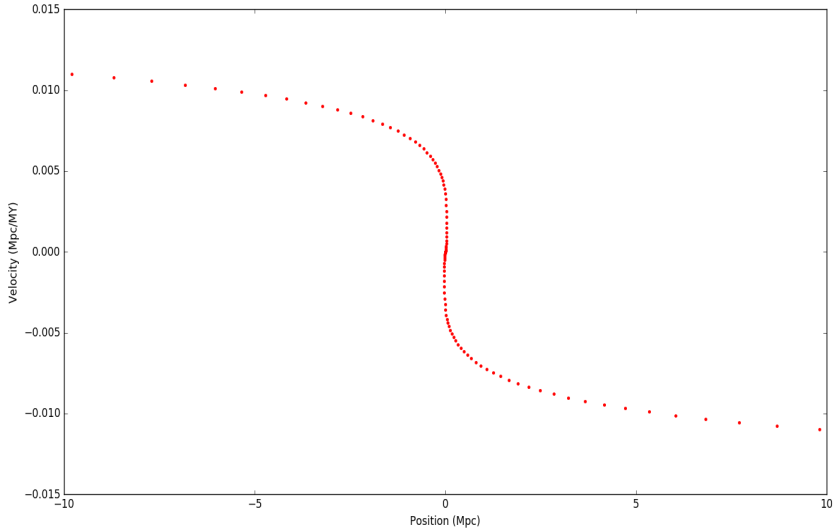

Figure 5.11: Phase space plot of study system after 130 million years.

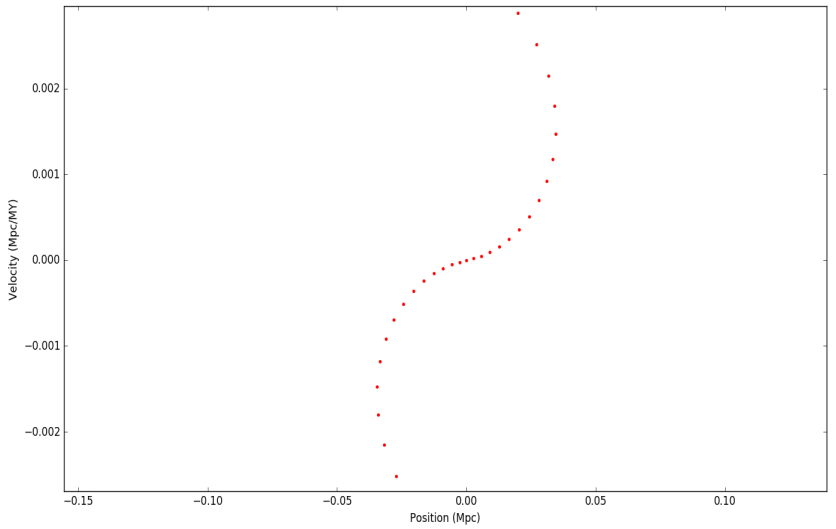

Figure 5.12: Zoomed in image of the study system after 130 million years.

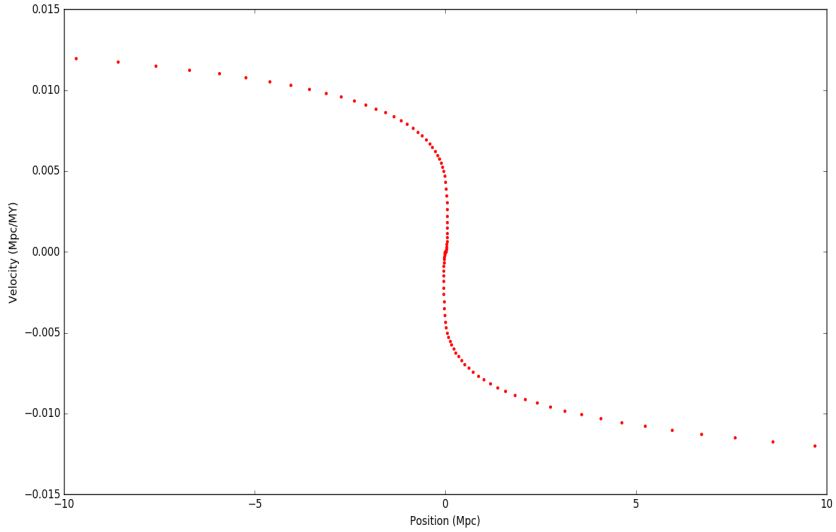

Figure 5.13: Phase space plot of study system after 140 million years.

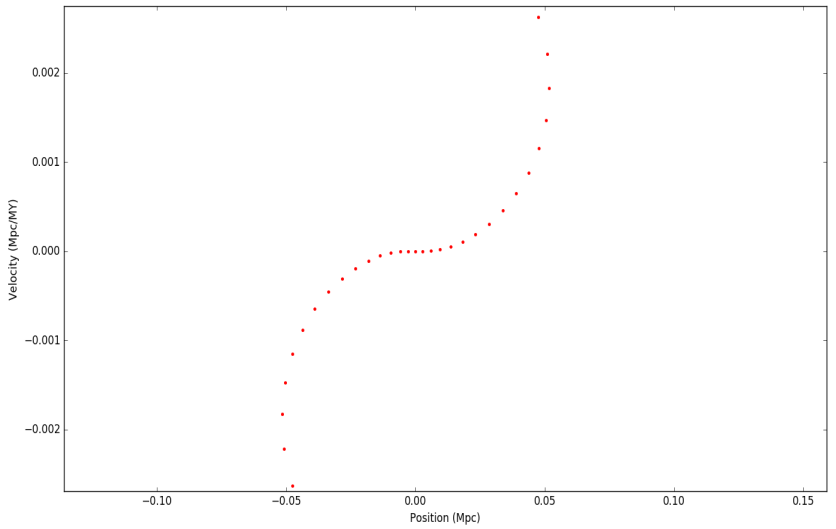

Figure 5.14: Zoomed in image of the study system after 140 million years.

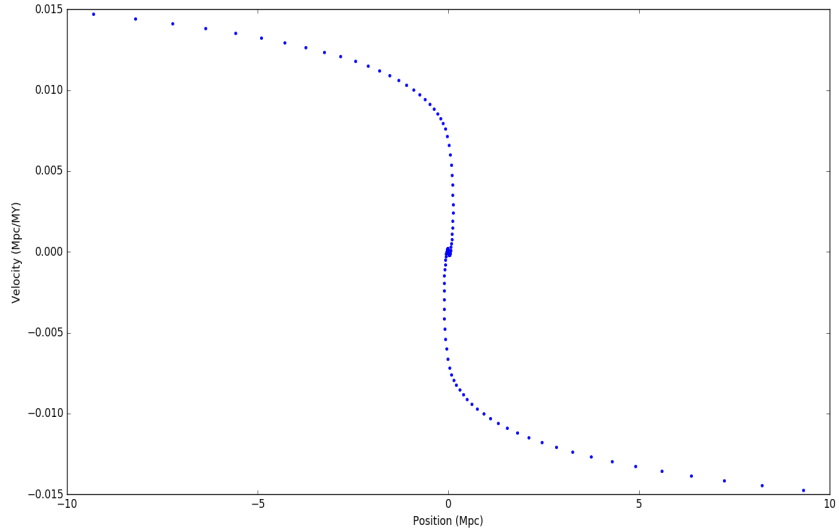

Figure 5.15: Phase space plot of study system after 160 million years.

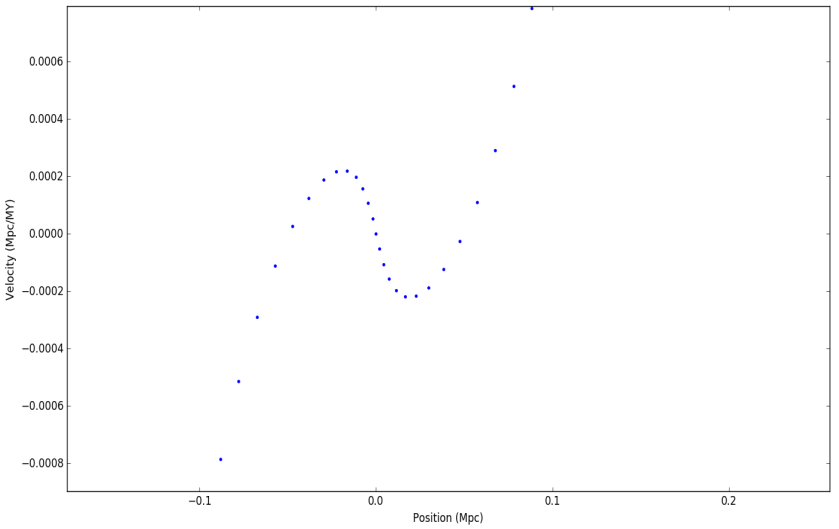

Figure 5.16: Zoomed in image of the study system after 160 million years.

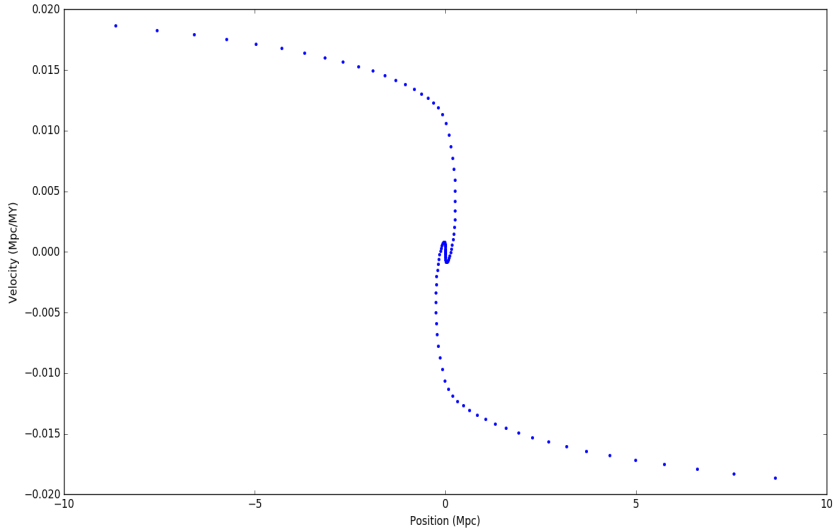

Figure 5.17: Phase space plot of study system after 200 million years.

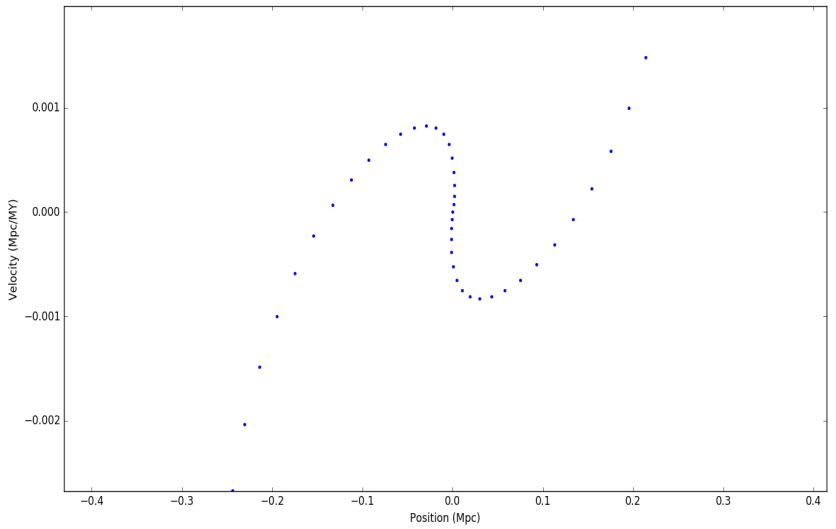

Figure 5.18: Zoomed in image of the study system after 200 million years.

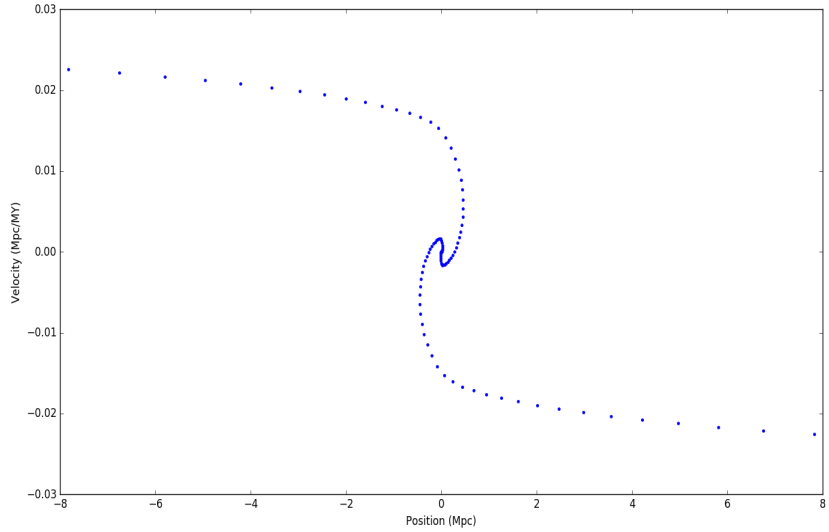

Figure 5.19: Phase space plot of study system after 240 million years.

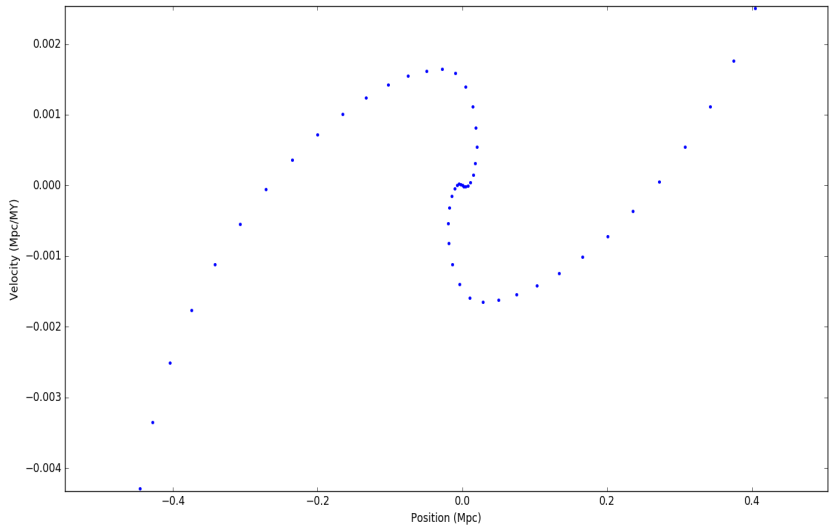

Figure 5.20: Zoomed in image of the study system after 240 million years.

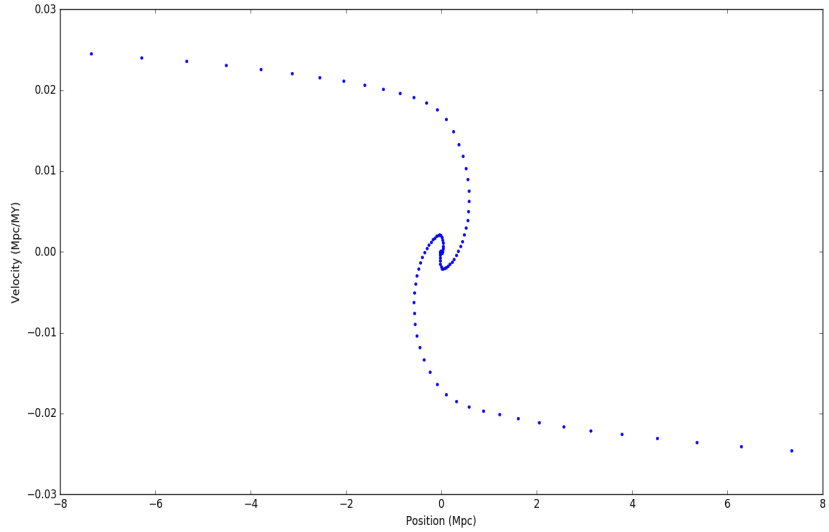

Figure 5.21: Phase space plot of study system after 260 million years.

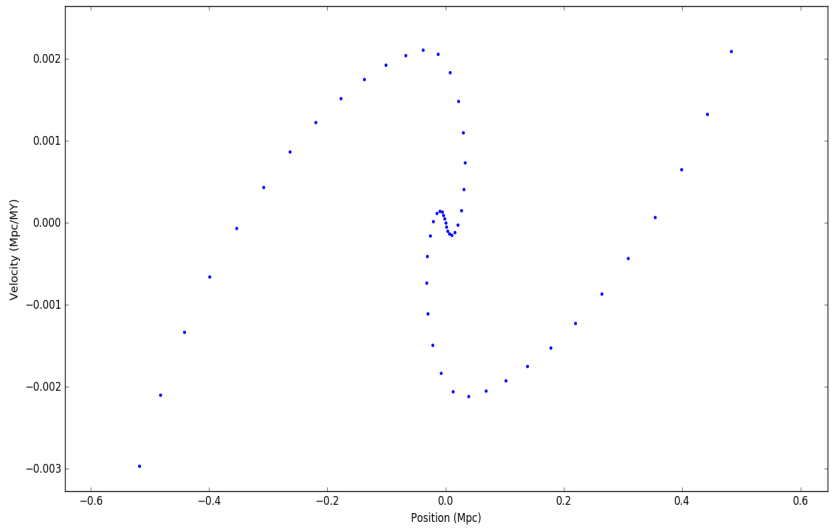

Figure 5.22: Zoomed in image of the study system after 260 million years.

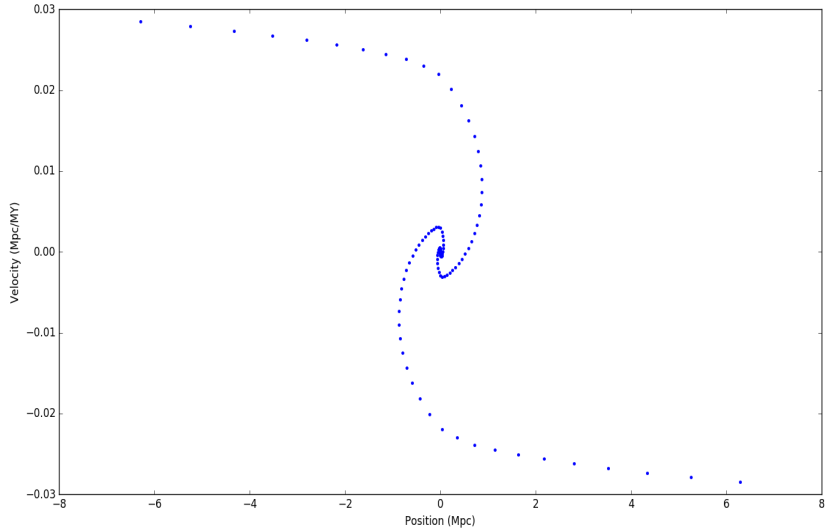

Figure 5.23: Phase space plot of study system after 300 million years.

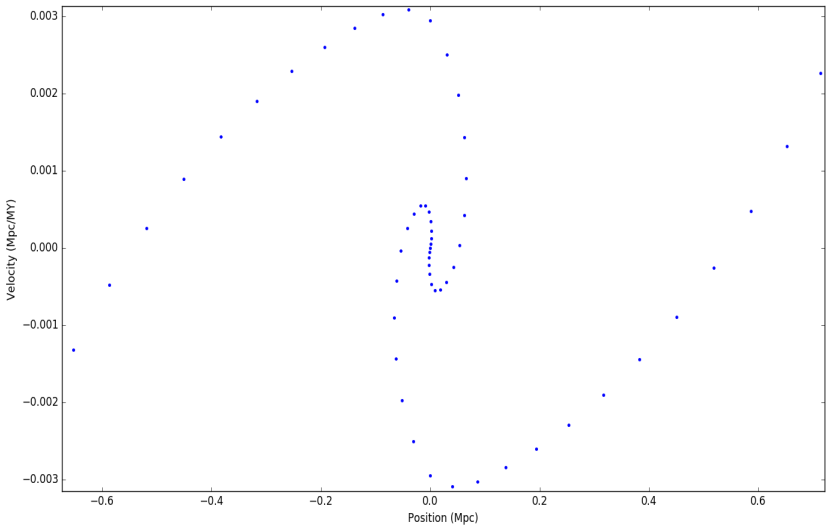

Figure 5.24: Zoomed in image of the study system after 300 million years.

Chapter 6

Testing the Origami Model

6.1 Testing the effect of no-stretch condition

Now that we have noticed that the real particles of the study system move in a manner which shows that the line of dark matter distribution is slowly folding, we write a test to see whether there is stretching of the dark matter line when the folding happens. If and when the line of dark matter distribution stretches, the distance between neighboring particles at the instant of folding will be greater than the distance that separated them in the initial set-up.

Let $x_k(t)$ and $x_{k+1}(t)$ be two neighboring real particles of the study system at some instant of time t in the systems evolution. The initial separation between the neighboring particles of the system is denoted by s_k.

$$s_k = x_{k+1}(0) - x_k(0) \tag{6.1}$$

The system of dark matter particles is allowed to interact gravitationally with the inhomogeneity while the boundary conditions are applied to it, for a fixed amount of time. At every time step when the position and velocity of the particles of the system are found using Euler's approximation method, the change in the distance between neighboring particles will be kept track of. Let their positions at the next time step $t + \Delta t$ be $x_k(t + \Delta t)$ and $x_k(t + \Delta t)$. Then the separation between the two particles at this time step is denoted by

$$\delta x_k = x_{k+1}(t + \Delta t) - x_k(t + \Delta t).$$

$\delta x_k - s$ is a measure of change in distance of separation between the two neighboring particles at that instant of time, in the evolution of the system. To ensure that this measure of change is not affected by the change in signs associated with the positions of the particles, δx_k obtained as mentioned above is squared and then the value of its square root is taken. If the line does not undergo any stretching, then the measure of change in distance of separation between neighboring particles at a given instant will be zero.

Next, at each time step the relative change in distance of separation between neighboring particles, the stretch parameter D_k, is calculated. That is,

$$D_k = \frac{(\sqrt{(\delta x_k)^2} - s_k)}{s_k} \tag{6.2}$$

is obtained. A graph of relative change in distance of separation between neighboring particles versus particle index, is plotted. This plot reveals by what amount the separation between any two neighboring particles of the study system has changed as compared to the distance separating them initially. This plot will be a horizontal line at $D_k = 0$ if the line of dark matter does not stretch while undergoing origami-like folding.

6.2 Testing the stretching of the study system

In the previous chapter we saw and discussed the phase space plots of a toy system. It contained a study system made of 101 particles with 55 dummy particles on each side at the boundary of the study system . We saw that at and after time slices corresponding to a 100 million years, the line-like distribution of dark matter in the study system undergoes folding (See,figures from 5.7 to 5.14 in chapter 5). The system was next tested for stretching on undergoing folding while under the influence of the gravitational affects of dummy particles on which the no-stretch approximation of the Origami model was strictly imposed. The testing was done as described in the previous section of this chapter. The result of the test for the study system containing 101 particles is shown below. The real particles of this system took index value, k from 55 to 155. The distance between neighboring particles for $k = 55$ to 155, in the initial state of the system (time = 0 s) was recorded when the initial positions of the particles are assigned to each

particle. The distance of separation between neighboring particles (for particles with index k from 55 to 155) at time corresponding to each time slice (100 million years to 140 million years) was also recorded. From these values, the stretch parameter D_k is obtained as explained in the previous section. Since the stretch parameter D_k depends on the positions of the particles calculated using the Euler's approximation method, it would be good to know the order of error associated with each time step due to the approximation method used. It has already been mentioned in chapter 3 section 3.2.1,that the order of error per time step of the Euler's method for the system studied will be $(0.01)^2$. The magnitude of acceleration experienced by each particle at the 300^{th} time slice was found to be in the order of 10^{-5}. Thus the error associated with the calculation of positions of the particles at the 300^{th} time slice is found to be equal to 10^{-5} Mpc for each particle, i.e., an error of 10 pc per particle due to the Euler's approximation method. A plot of D_k versus index k for the study system at different time slices is shown below:

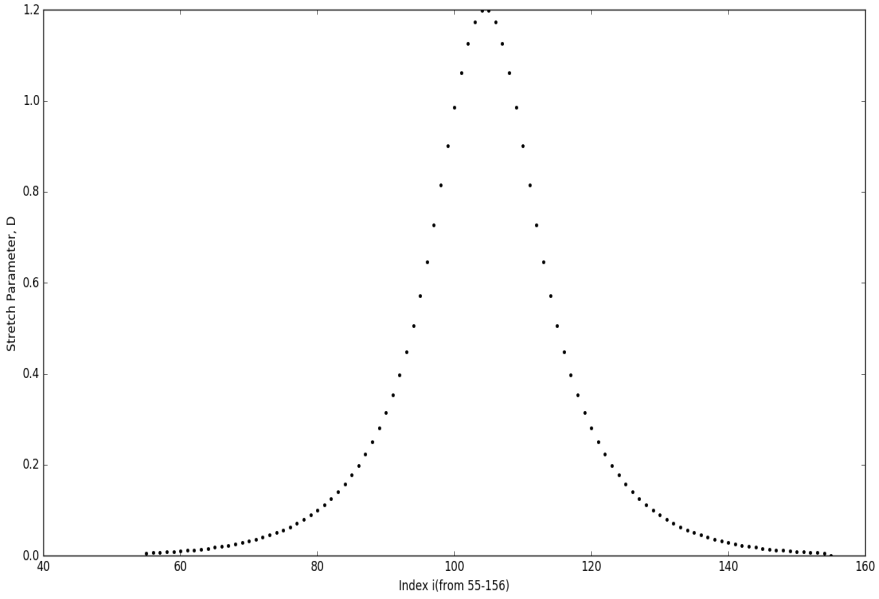

Figure 6.1: Stretch parameter D_k verses particle index k.
This plot is based on the position values of particles corresponding to 100 million years.

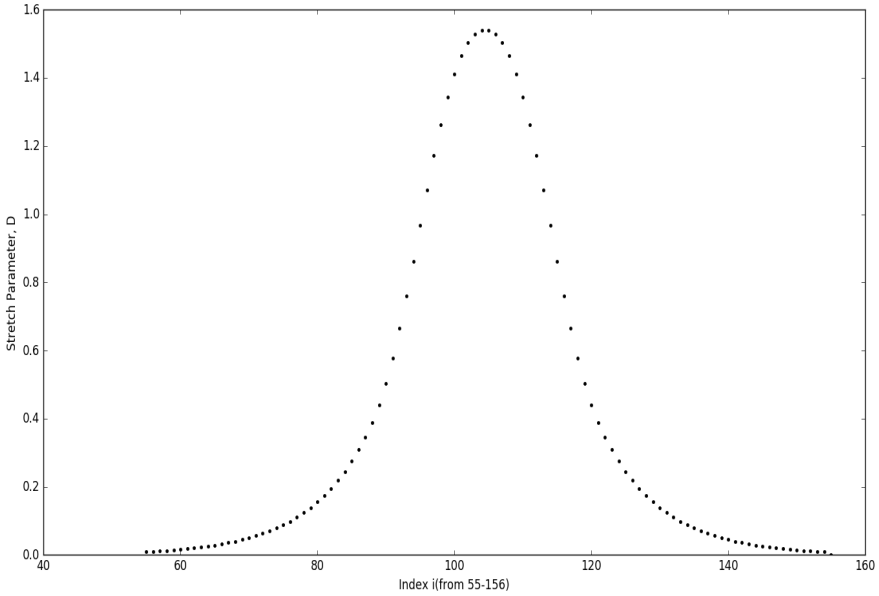

Figure 6.2: Stretch parameter D_k verses particle index k.
This plot is based on the position values of particles corresponding to 120 million years.

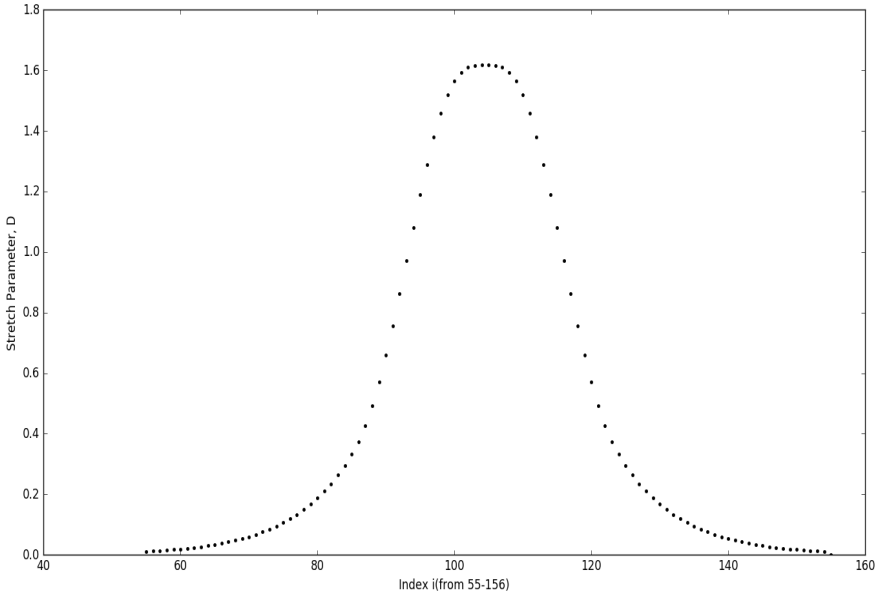

Figure 6.3: Stretch parameter D_k verses particle index k.
This plot is based on the position values of particles corresponding to 130 million years.

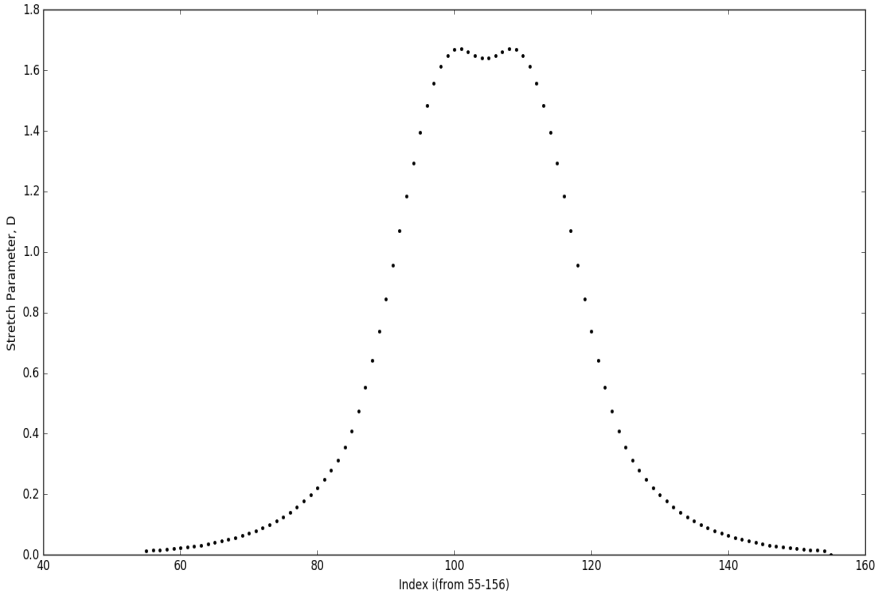

Figure 6.4: Stretch parameter D_k verses particle index k.
This plot is based on the position values of particles corresponding to 140 million years.

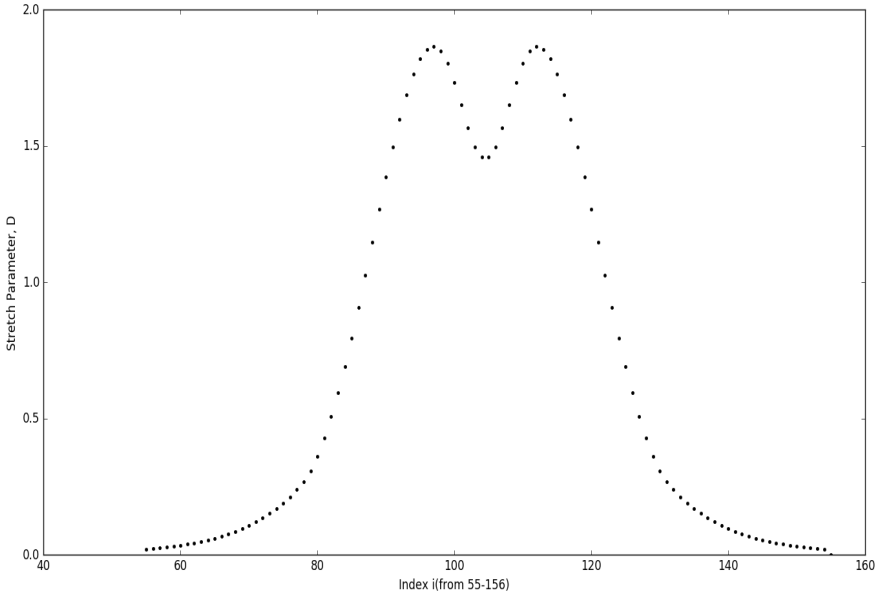

Figure 6.5: Stretch parameter D_k verses particle index k.
This plot is based on the position values of particles corresponding to 160 million years.

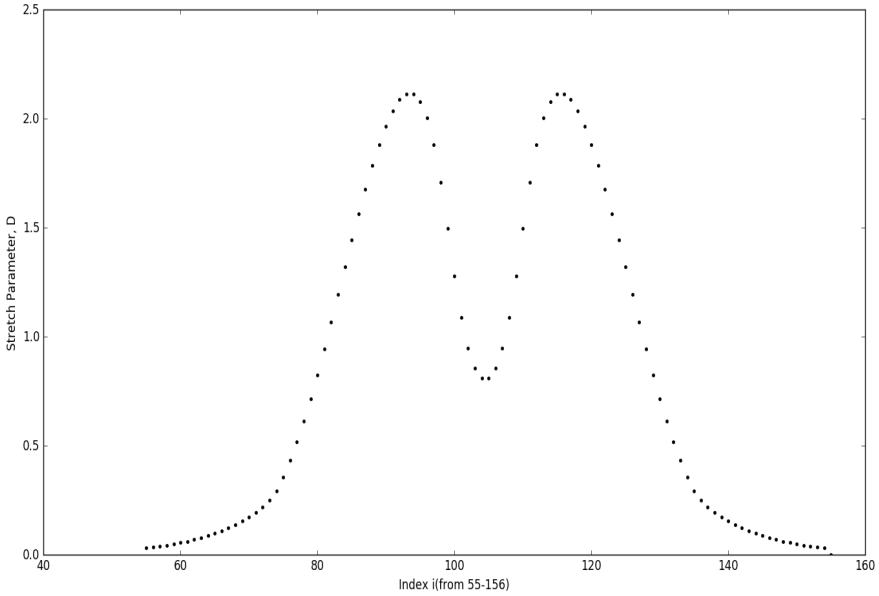

Figure 6.6: Stretch parameter D_k verses particle index k.
This plot is based on the position values of particles corresponding to 200 million years.

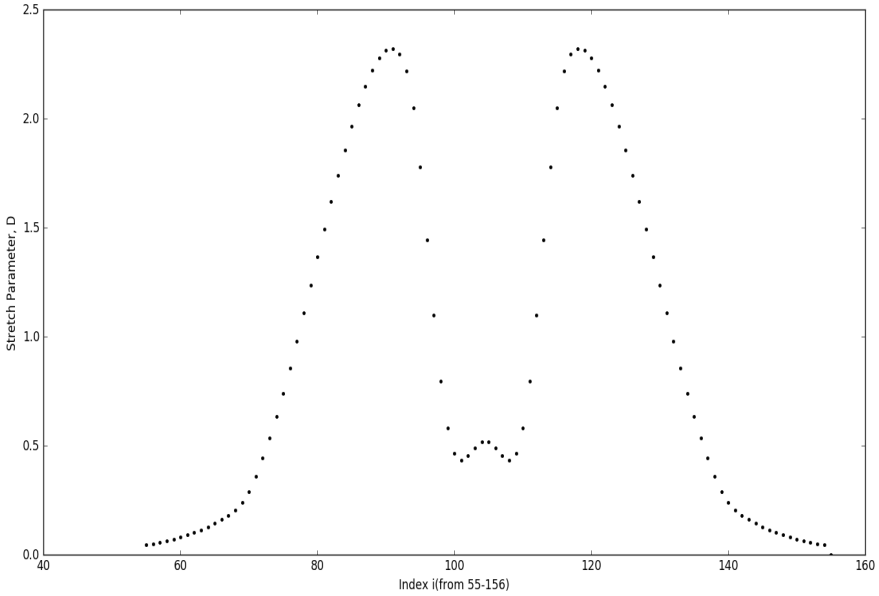

Figure 6.7: Stretch parameter D_k verses particle index k.
This plot is based on the position values of particles corresponding to 240 million years.

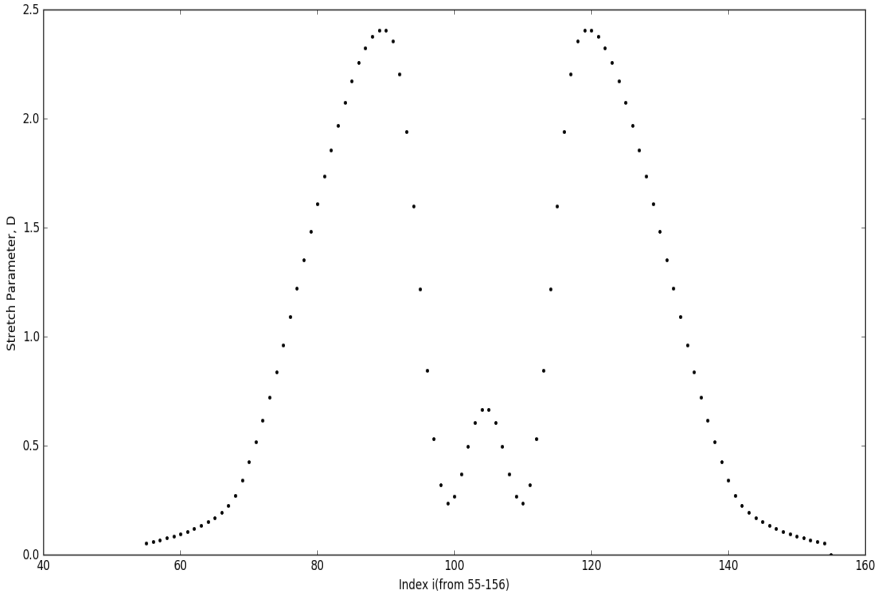

Figure 6.8: Stretch parameter D_k verses particle index k.
This plot is based on the position values of particles corresponding to 260 million years.

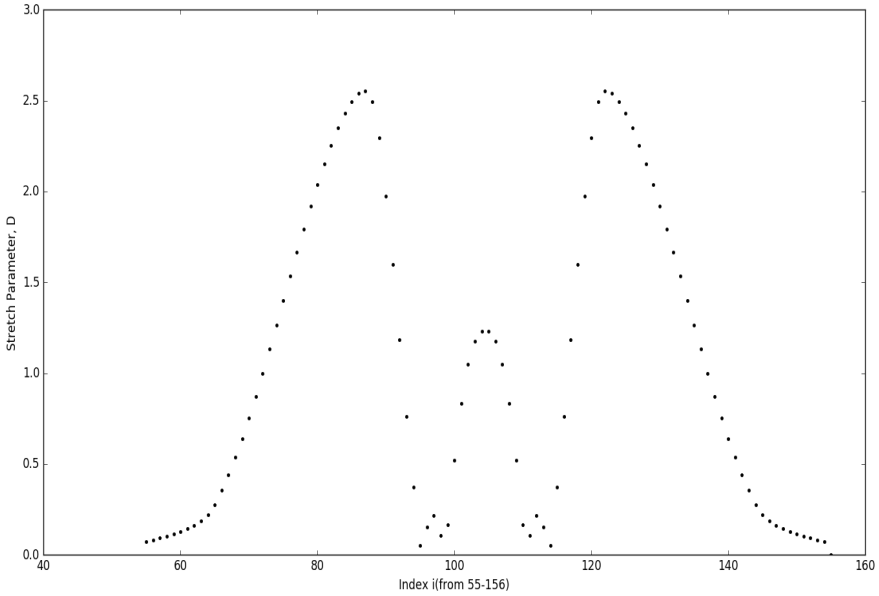

Figure 6.9: Stretch parameter D_k verses particle index k.
This plot is based on the position values of particles corresponding to 300 million years.

Chapter 7

Interpretation of Results and Discussion

7.1 Interpretation of results

At the end of chapter 4 section 4.3, we summarized the way in which we would like to meet the objective of this project undertaken, by posing a set of questions which will be answered in this section.

The answer to the first question is clearly depicted in the phase space plots of the study system in chapter 5, from figure 5.7 onwards. We can clearly see that, as study system evolved with time, the line-like distribution of dark matter in one dimension does fold significantly. And these foldings become more clearly visible in the phase space plot of the study system, with increasing amount of time for which it is allowed to evolve.

The second question is answered by means of the stretching parameter D versus particle index plots in chapter 6, section 6.2. The line-like distribution of dark matter is found to start folding from 100 million year into its evolution. We see from the comparison of figures in chapter 5 of the study systems phase plots at various time slices, with their corresponding stretch parameter versus particle index plots in chapter 6 section 6.2 (see figures 5.7 to 6.9) that, when the study system first folds, from a 100 million years to 130 million years into its evolution the distance between neighboring particles at the center of the study system steadily increases. This implies that the line-like distribution undergoes stretching.

As the amount of folding becomes more significant, at around 140 million years the stretching between neighboring particles at the center of the system reduces and two peaks are seen to form corresponnding to region between creases that occur when the distribution folds in its phase space. As the sytem is allowed to evolve further in time, we see that the distance between neighboring particles in regions between creases keeps on slowly increasing while the distance between neighboring particles at the center of the study system slowly decreases and approches its initial value. This indicates that the line-like distribution increasingly stretches in regions between the creases while the central part compresses and slowly returns to its initial state. This behavior seems to continue until the distribution undergoes one complete fold (till the end of nearly 230 million years into its evolution).

But when the system starts folding for the second time at around 240 million years, we see the distance between neighboring particles at the center of the study system increase again as does the distance between the neighboring particles in regions between the first creases formed (see figure 6.7), indicating that the central region of the distribution seems to be stretching again as it did when it first started folding. From figure 6.8 we can clearly make out the region of particles that are a part of the creases formed due to folding, as creases correspond to regions of the distribution where the distance between neighboring particles is the closest after undergoing folding. As the system evolves in time we also notice that on an overall, the stretching parameter has been slowly and steadily increasing for certain other regions mentioned above.

In figure 6.9 we can clearly see how more creases are formed as the central regions folds even further (see figure 5.24, to understand the situation a little better.) So, in our study system we see that the line-like distribution increasingly stretches in certain non-central regions while the central region switches between being compressed and stretched as the system undergoes more and more foldings.

For this study, the system has been allowed to evolve for 300 million years. At this point of time the study system is in the process of undergoing folding for the second time and from figure 6.9 we can clearly see that the highest value of stretch paramater lies a little above 2.5. The decision of whether this amount of stretching of the line-like distribution of dark matter in the study system under the imposition of no-stretch approximation

at the boundaries of the system, will strongly depend on the cut-off value of stretch parameter D that we settle for.

For a chosen cut-off value of the stretch parameter, whether or not the origami model can be used for study of structure formation will greatly depend on how many particles of the system will have a stretch parameter below the cut-off at any point of time in the systems evolution. For example, if we settle for a stretch parameter cut-off value of 3 then, clearly from figure 6.9, as no region in the plot has a stretch parameter beyond 3, we can say that the no-stretch condition of the origami model still holds good and the model can be safely used to study structure formation. But a stretch parameter cut-off should be as small as possible. Hence a cut-off of value of 1.5 would be better than 3. Then, for figure 6.9, we see that since a relatively large portion of the study system still has stretch parameter less than or equal to 1.5, the no-stretch approximation still holds good for the most part and the origami model can still be of use to us for the study of structure formation. And since a major portion of the entire system (including the dummy particles for which D is strictly set to zero) has a stretch parameter well below 1.5, and only certain regions with fewer particles go beyond the cut-off by only a small amount, we can still make use of the origami model to atleast be able to classify what kind of structure is expected to form in a certain region, for a particular kind of allowed folding pattern of the origami model (as it is applicable for most parts of the study system to explain structure formation).

A stretch parameter of 1 represents a situation where the distance between any two neighboring particles of the study system at a given instant of time in its evolution is twice the intial distance of separation between them i.e., a situation with 100 percent stretching. This makes a stretch parameter of 1 a reliable choice as a cut-off value. For a stretch parameter cut-off of 1, from figure 6.9, major part of the entire system still has a stretch parameter below 1. Behavior in these regions of the line-like distribution of dark matter can be studied using the origami model. But for regions corresponding to stretch parameters that are much greater than 1, applying the origami model for study of structure formation will not be a good idea.

7.2 Further discussion

The work done in this project undertaken is a crude test for the origami model proposed to explain the large scale structure formation in the universe. There is much scope for improvement of this study. A few points for improvement are mentioned below:

- The study mainly focuses on the simplest case scenario - a one dimensional universe with a line-like distribution of dark matter. One can take a step or two further and try to move into a higher dimensional picture of the situation.

- This study has made use of just one kind of study system in which the spacing parameter l (refer 4.2) has been arbitrarily chosen to be 0.12. One can further the scope of this study by chosing to see how varying l effects the behavior of the study system. This will help determine the initial conditions of systems for which the Origami model holds good.

- One of the best ways to improve this study would be to use better numerical approximation methods which are far more faster and reliable than the simple Eulers method used here.

- The number of dummy particles for the study system here was also arbitrarily chosen. And this entire study has been based on Newton's theory of gravity. But one can widen the scope of this study by making use of general theory of relativity, which provides a more accurate picture of gravity. On replacing Newton's theory of gravity with general relativity one can increase the size of the study system and depending on the computational power they can afford, one can also carry out an improved version of this study with a bigger system of N particles.

Of course, all the above mentioned points will make this study a lot more difficult while demanding time and effort. But they can be incorporated one step at a time into this study to be able to produce more reliable results.

Bibliography

[1] Mark C Neyrinck and Sergei F Shandarin. Tessellating the cosmological dark-matter sheet: origami creases in the universe and ways to find them. *arXiv preprint arXiv:1207.4501*, 2012.

[2] Martin White, Douglas Scott, and Joseph Silk. Anisotropies in the cosmic microwave background. *Annual Review of Astronomy and Astrophysics*, 32:319–370, 1994.

[3] Scott Dodelson. *Modern cosmology*. Academic press, 2003.

[4] Todd Duncan and Craig Tyler. *Your cosmic context: an introduction to modern cosmology*. Addison-Wesley, 2009.

[5] Varun Sahni and Peter Coles. Approximation methods for non-linear gravitational clustering. *Physics Reports*, 262(1-2):1–135, 1995.

[6] Donald G York, J Adelman, John E Anderson Jr, Scott F Anderson, James Annis, Neta A Bahcall, JA Bakken, Robert Barkhouser, Steven Bastian, Eileen Berman, et al. The sloan digital sky survey: Technical summary. *The Astronomical Journal*, 120(3):1579, 2000.

[7] Matthew Colless, Gavin Dalton, Steve Maddox, Will Sutherland, Peder Norberg, Shaun Cole, Joss Bland-Hawthorn, Terry Bridges, Russell Cannon, Chris Collins, et al. The 2df galaxy redshift survey: spectra and redshifts. *Monthly Notices of the Royal Astronomical Society*, 328(4):1039–1063, 2001.

[8] J.R. Gott. *The Cosmic Web: Mysterious Architecture of the Universe*. Princeton University Press, 2016.

[9] Peter AR Ade, N Aghanim, C Armitage-Caplan, M Arnaud, M Ashdown, F Atrio-Barandela, J Aumont, C Baccigalupi, Anthony J Banday, RB Barreiro, et al. Planck 2013 results. xxii. constraints on inflation. *Astronomy & Astrophysics*, 571:A22, 2014.

[10] PAR Ade, N Aghanim, M Arnaud, M Ashdown, J Aumont, C Baccigalupi, AJ Banday, RB Barreiro, JG Bartlett, N Bartolo, et al. Planck 2015 results-xiii. cosmological parameters. *Astronomy & Astrophysics*, 594:A13, 2016.

[11] Ya B Zel'Dovich. Gravitational instability: An approximate theory for large density perturbations. *Astronomy and astrophysics*, 5:84–89, 1970.

[12] John A Peacock. *Cosmological physics*. Cambridge university press, 1999.

[13] Mark C Neyrinck. Cosmological origami: Properties of cosmic-web components when a non-stretchy dark-matter sheet folds. *arXiv preprint arXiv:1408.2219*, 2014.

[14] Douglas Scott, Joe Silk, and Martin White. From microwave anisotropies to cosmology. *arXiv preprint astro-ph/9505015*, 1995.

PROJECT DETAILS

Student details			
Student Name	**Fiona Shalom D'Mello**		
Registration No.	**153103007**		
Email Address	**shalomdmello@gmail.com**		
Phone No.	**9481177267**		
Project Details			
Project Title	**Numerical Study of Large Scale Structure Formation of the Universe**		
Project Duration	**2016-2017**	Date of Submission	**29.04.2017**
Supervisor Details			
Supervisor Name	**Dr. Kazuyuki Furuuchi**		
Designation	**Associate Professor**		
Official Address	**Manipal Centre of Natural Sciences (MCNS), Manipal University, Manipal**		
Official Email Address	**kazuyuki.furuuchi@manipal.edu**	Phone No.	+918861934703